Supporting Information

Threading salen-type Cu- and Ni-complexes into one-dimensional coordination polymers: Solution versus solid state, and the size effect of the alkali metal ion

Alba Finelli [†], Nelly Hérault [†], Aurelien Crochet [‡], Katharina M. Fromm *[,†]

[†] Department of Chemistry, University of Fribourg (UNIFR), Ch. du Musée 9, 1700 Fribourg, Switzerland

[‡] FriMat, Department of Chemistry, University of Fribourg, Ch. du Musée 9, 1700 Fribourg, Switzerland.

Table of Contents

General

All experiments were performed in air and at RT. Ligand **H_2L** was prepared according to the procedure reported by Avecilla et al. previously. All chemicals were commercial products of reagent grade and were used without further purification. ^{1}H and ^{13}C measurements were carried out for the Ni–compounds with a Bruker 400 MHz spectrometer at ambient temperature, and chemical shifts are given in ppm with respect to the residual solvent peak. Mass spectra (ESI-TOF, positive mode) were recorded with a Bruker esquire HCT spectrometer with a DMF/ACN mixture as solvent. The UV/Vis spectra were recorded with a Perkin–Elmer Lambda 40 spectrometer. The crystallographic data of single crystals were collected with Mo-Kα radiation (λ = 0.71073 Å).

All measurements were performed at 200 K, or 250 K for the compounds **1'**, **2'** and **7'**, with Stoe IPDS-II or IPDS-II T diffractometers equipped with Oxford Cryosystem open-flow cryostats. Single crystals were picked under the microscope, and placed in inert oil. All crystals were mounted on loops and all geometric and intensity data were taken from one single crystal. The absorption corrections were partially integrated in the data reduction procedure. The structures were solved and refined using full-matrix least-squares on F^2 with the SHELX-2014 package. All atoms (except hydrogen atoms) were refined anisotropically. Hydrogen atoms were refined where possible, and otherwise added using the riding model position parameters. Crystallographic data can be found in the Supporting Information **(see Table S1)**. CIF files can be obtained from the Cambridge Crystallographic Data Centre, **CCDC-1497630 (1), CCDC-1518363**

(1'), CCDC-1497673 (2), CCDC-1518361 (2'), CCDC-1497674 (4), and CCDC-1497675 (5), CCDC-1497676 (6), CCDC-1497677 (7), CCDC-1518362 (7'), CCDC-1497678 (8), CCDC-1497679 (9), CCDC- 1497680 (10). Copies of these data can be obtained free of charge from the Cambridge Crystallographic Data Centre via www.ccdc.cam.ac.uk or e-mail, depos-it@ccdc.cam.ac.uk. Powder X-ray spectra were collected on a Stoe STADIP using Cu-Kα1 radiation (1.5406 Å) using a Mythen detector.

Synthesis

Synthesis of ligand H_2L. The compound **H_2L** was synthesized as described in the literature.[55] Ethane-1,2-diamine (0.395 g, 0.875 ml, 6.57 mmol) was added to a solution of *o*-vanillin (2g, 13.15 mmol) in methanol (1000 ml). After stirring the mixture for 2h at room temperature, the yellow precipitate was filtrated, washed with methanol and, diethyl ether to be dried under vacuum to produce the ligand **H_2L** (4.02 g, 94%). ^{1}H NMR (400 MHz, DMSO): δ 3.76 (s, 6H), 3.92 (s, 4H), 6.77-6.81 (t, *J*= 7.9 Hz, 2H), 6.98-7.2 (dd, *J*=71.7, 1.4Hz, 4H), 8.56 (s, 2H), 13.52 (s, 2H). ESI-MS (m/z): 329.1 $[1+H]^+$.

Synthesis of complex [LCu(H_2O)] "LCu". The complex **LCu** was synthesized as described in the literature.[63] A solution of $Cu(OAc)_2{\cdot}H_2O$ (152 mg, 0.761 mol) was added to a solution of **H_2L** (250 mg, 0.761 mol) in methanol (30 ml). The mixture turned dark green immediately. After the mixture was stirred for 3h at room temperature, the precipitate was collected by filtration and dried under vacuum to produce the complex **LCu** (278 mg, 90%). Green lozenge-like single crystals suitable for X-ray crystallographic analysis were obtained by recrystallization in DMF. ESI-MS (m/z): 408.0 $[M+H]^+$.

Synthesis of complex LNi. The complex **LNi** was prepared by adaptation of a literature procedure.[64] A solution of $Ni(OAc)_2{\cdot}\ 4H_2O$ (148.5 mg, 0.761 mmol) was added to a solution of **H_2L** (250 mg, 0.761 mmol) in methanol (30 ml). The mixture turned dark red immediately. After the mixture was stirred for 3h at room temperature, the precipitate was collected by filtration and dried under vacuum to produce the complex **LNi** (280 mg, 92%). Red, needle-like single crystals suitable for X-ray crystallographic analysis were obtained by recrystallization from DMF. ^{1}H NMR (400 MHz, DMSO-d_6): δ(ppm) 3.41 (s, 4H), 3.69 (s, 6H), 6.44-6.45 (t, *J*= 7.8 Hz, 2H), 6.76-7.78 (dd, *J*=7.6, 1.5 Hz, 2H), 6.85-6.88 (dd, *J*=8, 1.6 Hz, 2H), 7.87 (s, 2H). ESI-MS (m/z): 385.0 $[M+H]^+$.

Figure S1: Crystal structure LCu (above) and LNi (below), showing the square pyramidal coordination of the copper and the square planar coordination of the nickel in the N_2O_2 site. H-atoms except for water are omitted for clarity.

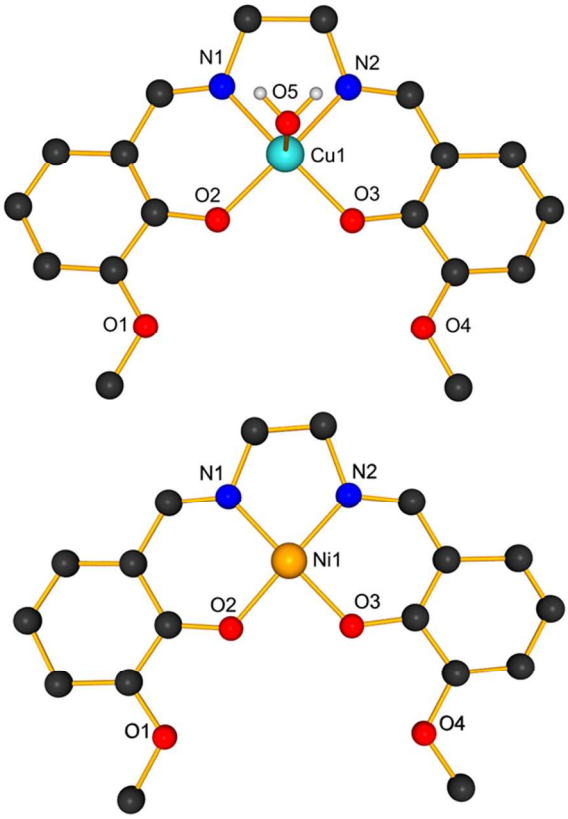

UV-Vis and NMR Titration of the free ligand H_2L

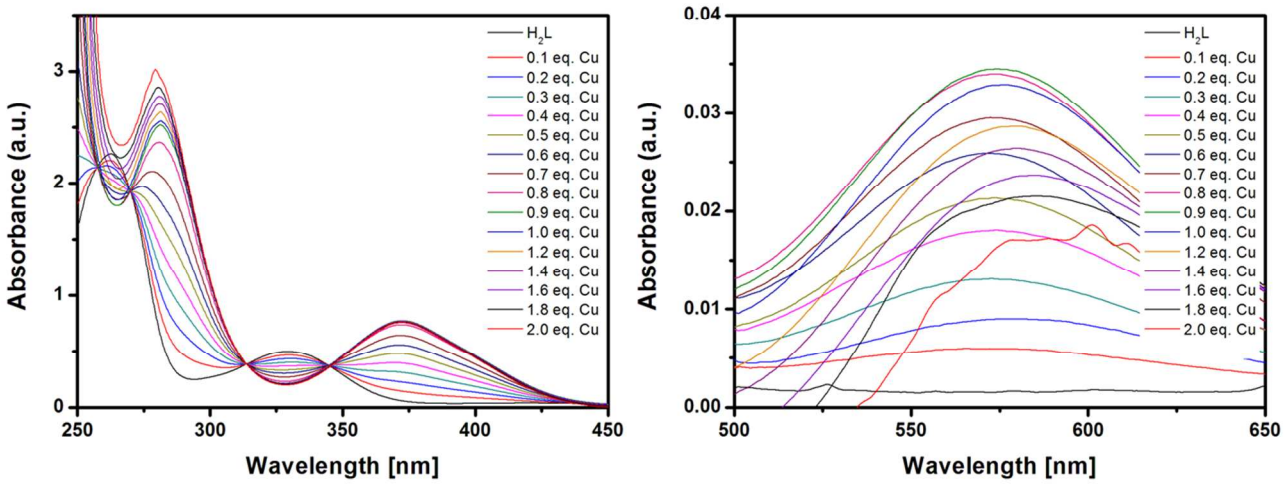

Figure S2 : UV-Vis spectral changes of the free ligand H_2L in ACN (0.1mM) upon the addition of a solution of $Cu(OAc)_2$ in MeOH.

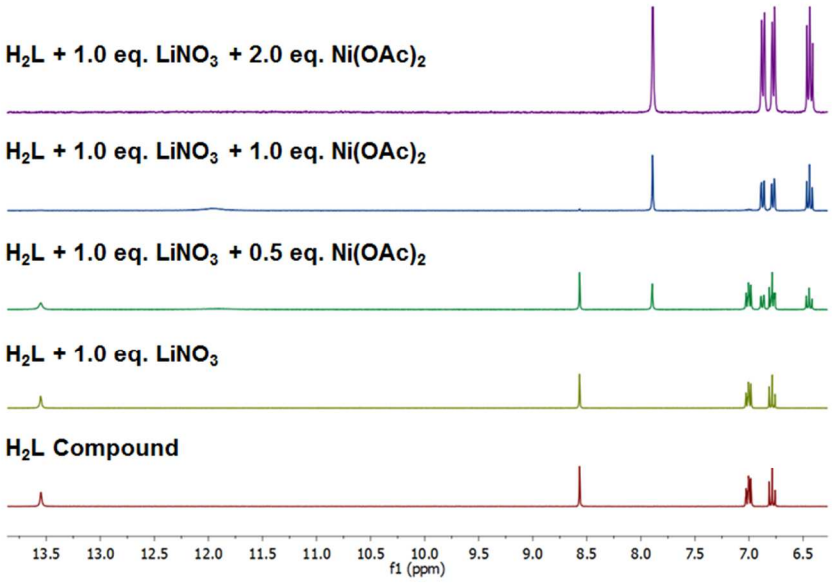

Figure S3 : ^1H NMR titration of the H_2L free ligand by adding inversely first up to two equivalents M_2 ($LiNO_3$) and then M_1 ($Ni(OAc)_2$), with the complex formation occurring only upon addition of M_1 and reaching completion after 1 equivalent of M_1.

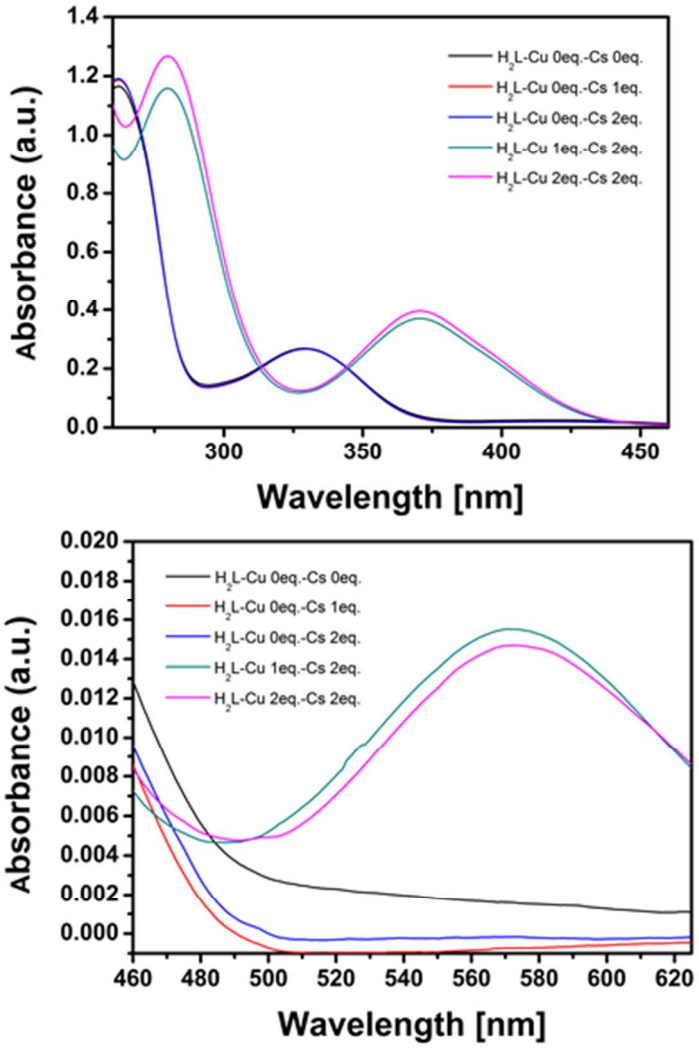

Figure S4: UV-Vis titration of the H_2L free ligand by adding first M_2 ($CsNO_3$) and then M_1 ($Cu(OAc)_2$), seeing the formation of the complex by the addition of the first M_1 metal ion. Up to the addition of two equiv. of alkali metal ion, the spectrum remains unchanged; only after the addition of the transition metal ion, is the new specie formed.

Template effect of the M_1L. The effect of the addition sequence between the transition metal M_1 and alkali metal M_2 with the ligand **H_2L** was investigated on the complex formation, performing ^1H NMR and UV-Vis studies. While the addition of the transition metal ion M_1 (= Cu(II) or Ni(II)) leads to an immediate shift of the NMR-signals for the Ni(II) compound, with respect to of the UV-Vis absorption bands for the Cu(II) compound, no change is observed when an alkali metal ion M_2 alone is added to the ligand alone. The electronic absorption.

Scheme S1: The two possible synthetic routes.

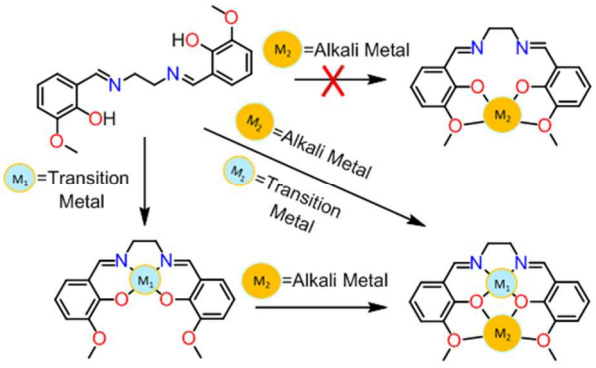

The spectrum of the free ligand **H_2L** presents two main bands; one broad band at ca. 340 nm assigned to an

n→π* transition at the azomethine group, and a band at ca. 250 nm probably associated to the transition involving the extended delocalized π- system localized on the C=N group and the aromatic ring[55] .The electronic absorption spectrum remains unchanged after the addition of up to 2.0 eq. of M_2. Also, if the alkali metal ion is added first, followed by the addition of 0.5, 1, or 2 equivalents of the transition metal ion M_1, spectral changes on the NMR- (**Fig. S3**), or UV-Vis-spectrum (**Fig. S4**) are only observed upon addition of the transition metal ion. Hence, the transition metal ion is required to induce the bending of the ligand and to preorganize the O_2O_2 cavity allowing it to host the alkali metal ion. Even the deprotonation of the two alcohol functions does not allow the formation of a stable enough alkali metal ion complex in solution (at least not on the NMR time-scale) without the presence of the transition metal ion. This template effect by the chelation of the copper(II) or nickel(II) is clearly required to prearrange the ligand like a tweezer and to bind the alkali metal ion in the O_2O_2 coordination site (Scheme 2).

UV-Vis Titration of the metallohost LCu

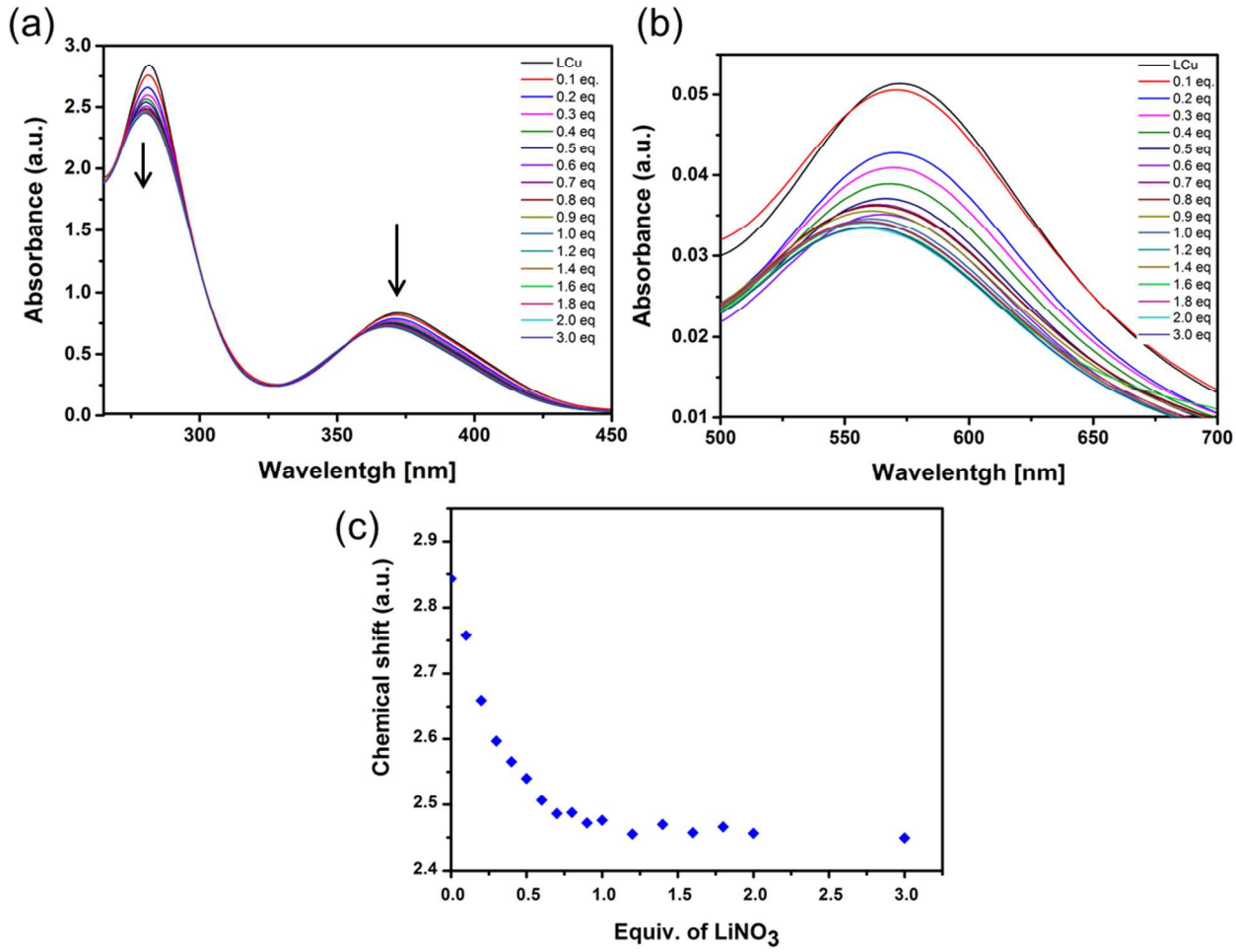

Figure S5 : UV-Vis spectral changes of the metallohost LCu in ACN upon the addition of a solution of $LiNO_3$ in DMSO.

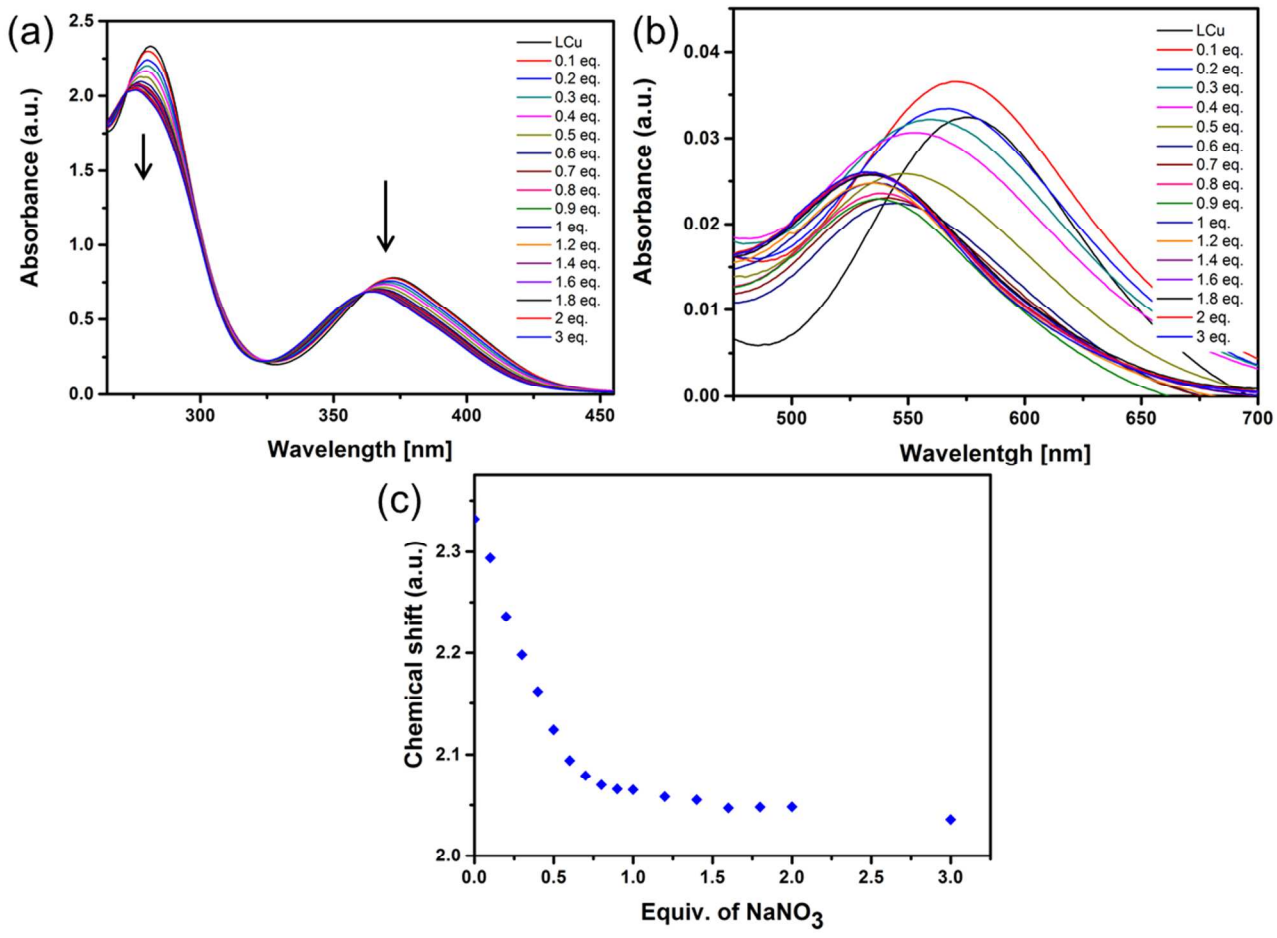

Figure S6 : UV-Vis spectral changes of the metallohost LCu (0.1 mM) in ACN upon the addition of a solution of $NaNO_3$ in DMSO.

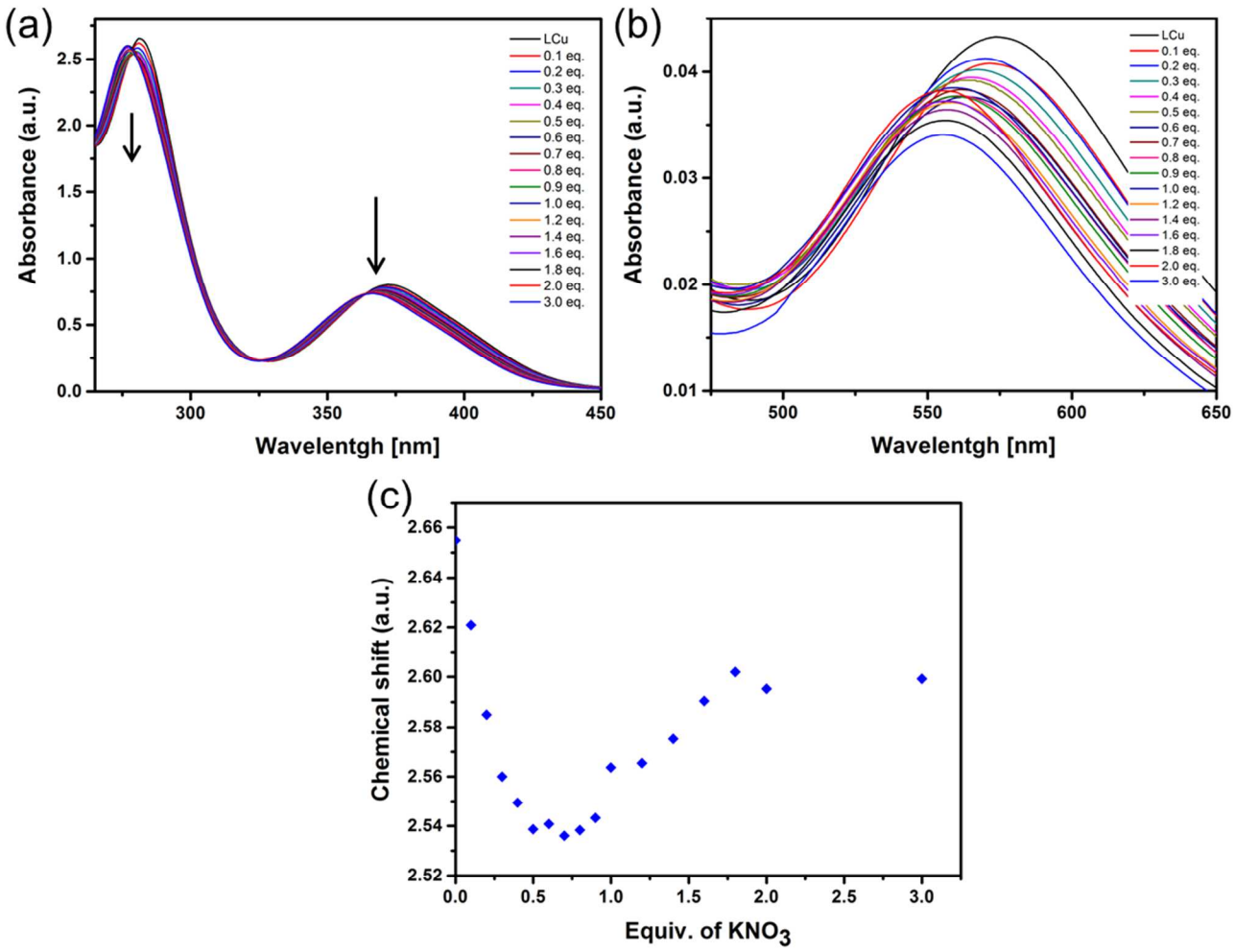

Figure S7: UV-Vis spectral changes of the metallohost LCu (0.1 mM) in ACN upon the addition of a solution of KNO_3 in DMSO.

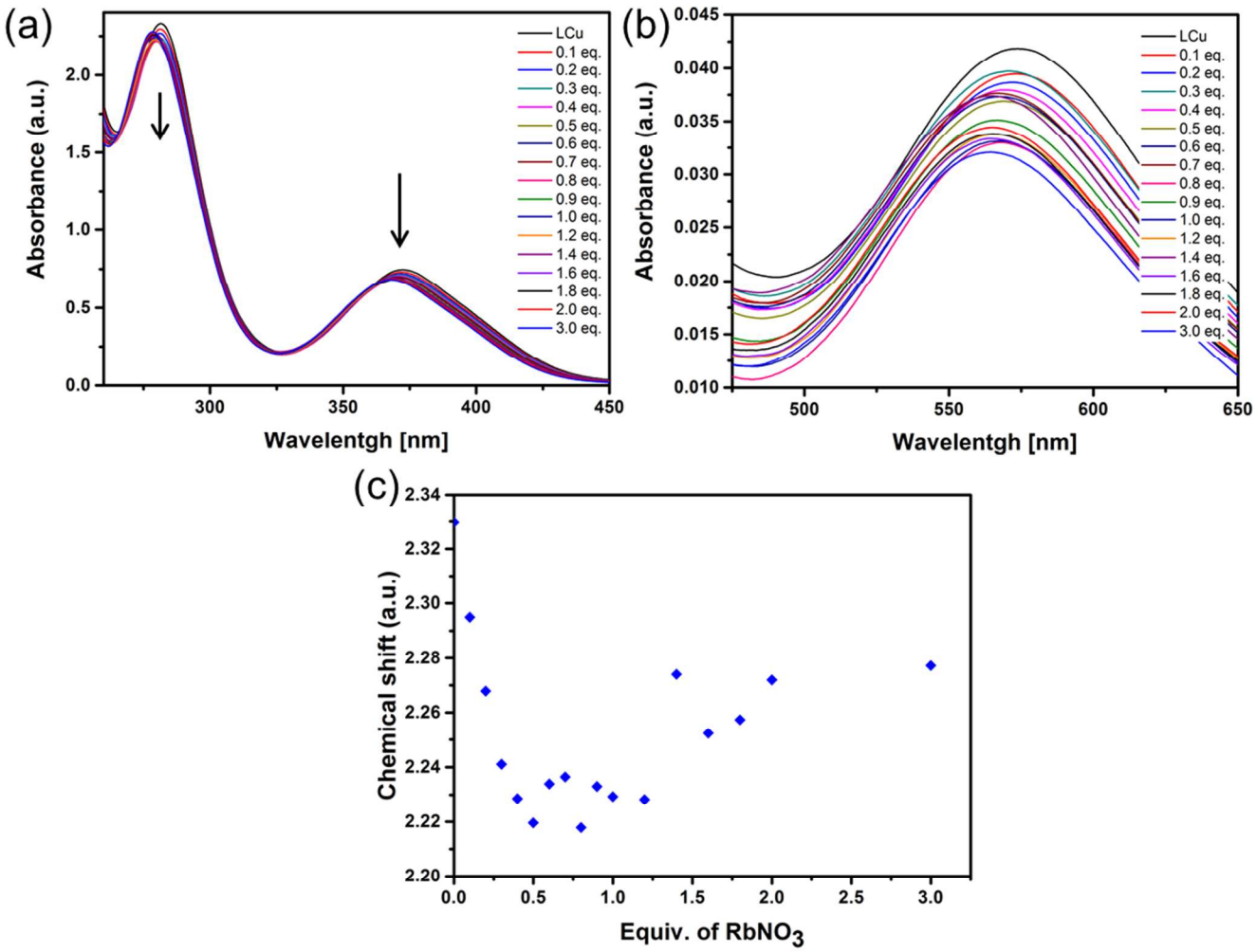

Figure S8: UV-Vis spectral changes of the metallohost LCu (0.1 mM) in ACN upon the addition of a solution of $RbNO_3$ in DMSO.

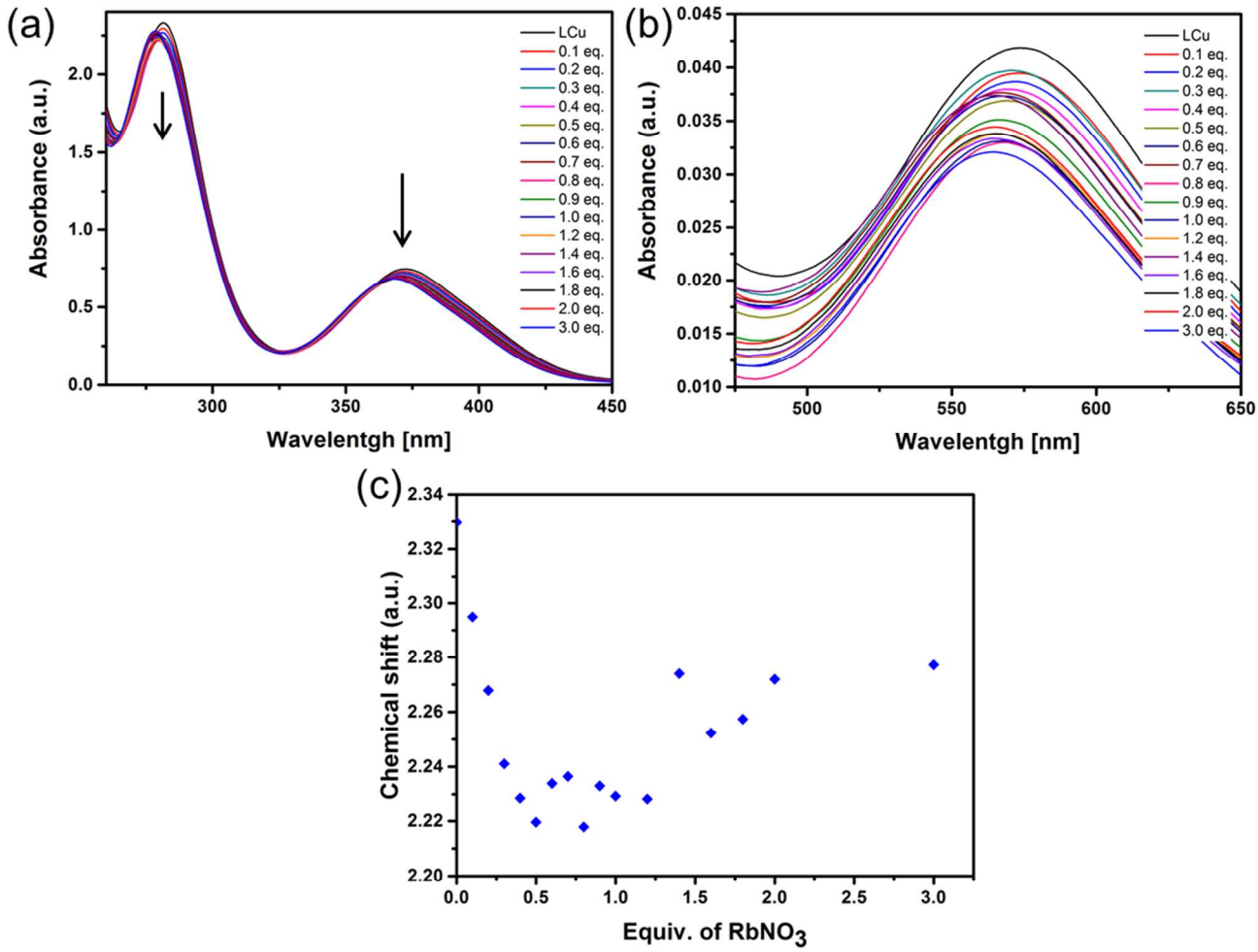

Figure S9: UV-Vis spectral changes of the metallohost LCu (0.1 mM) in ACN upon the addition of a solution of $CsNO_3$ in DMSO.

NMR spectrum of H_2L and LNi

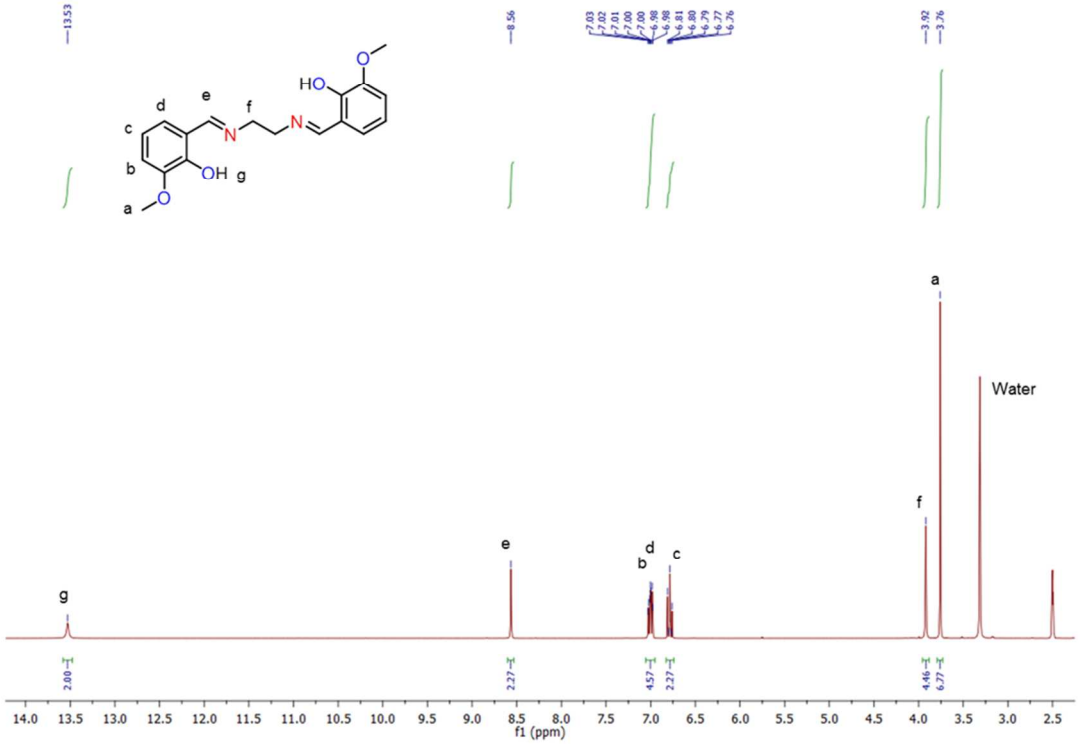

Figure S10: ^{1}H NMR spectrum of H_2L (400 MHz, DMSO-d_6, 0.02 M).

NMR Titration of metallohost LNi

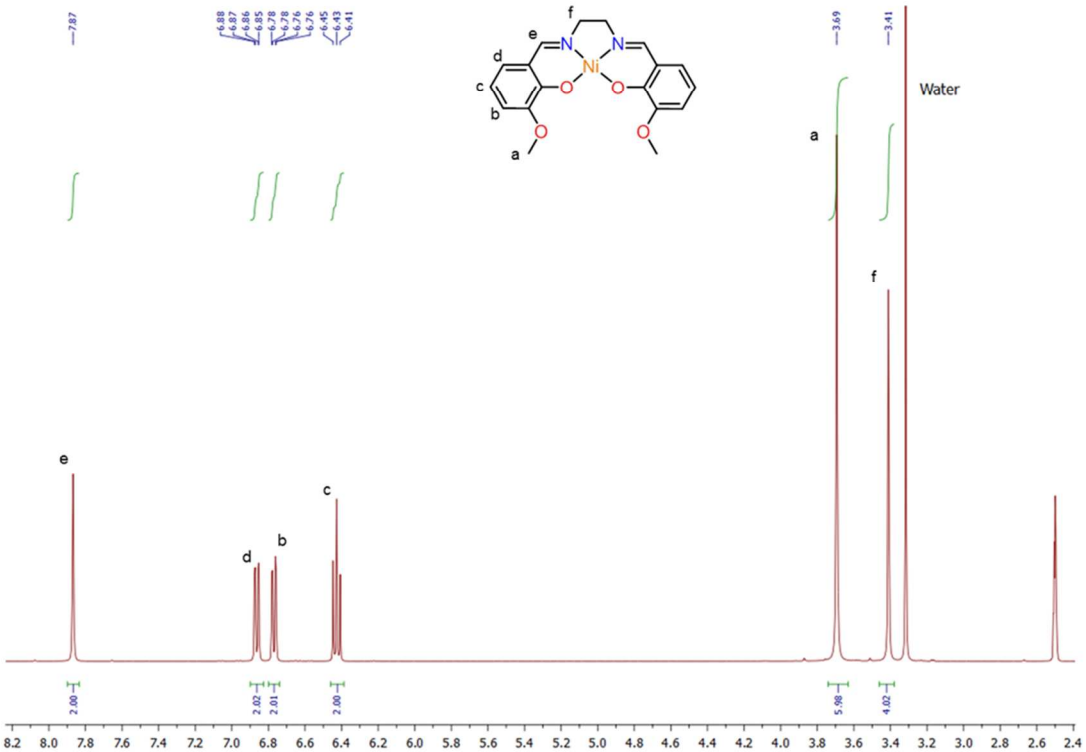

Figure S11: ^{1}H NMR spectrum of LNi (400 MHz, DMSO-d_6, 0.02 M).

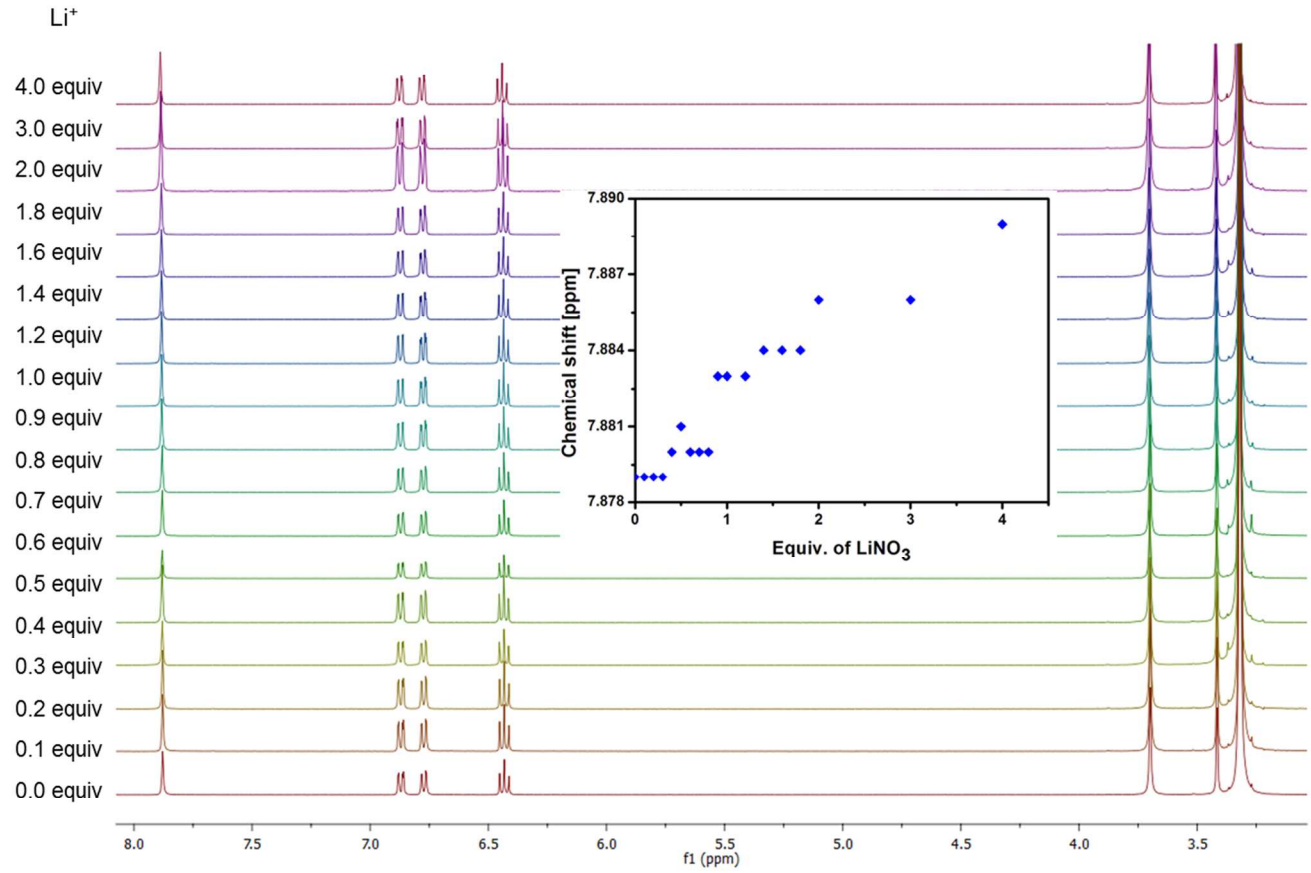

Figure S12: ^{1}H NMR spectral changes of the metallohost LNi (400 MHz, DMSO-d_6, 0.02 M) upon the addition of $LiNO_3$ in deuterated DMSO.

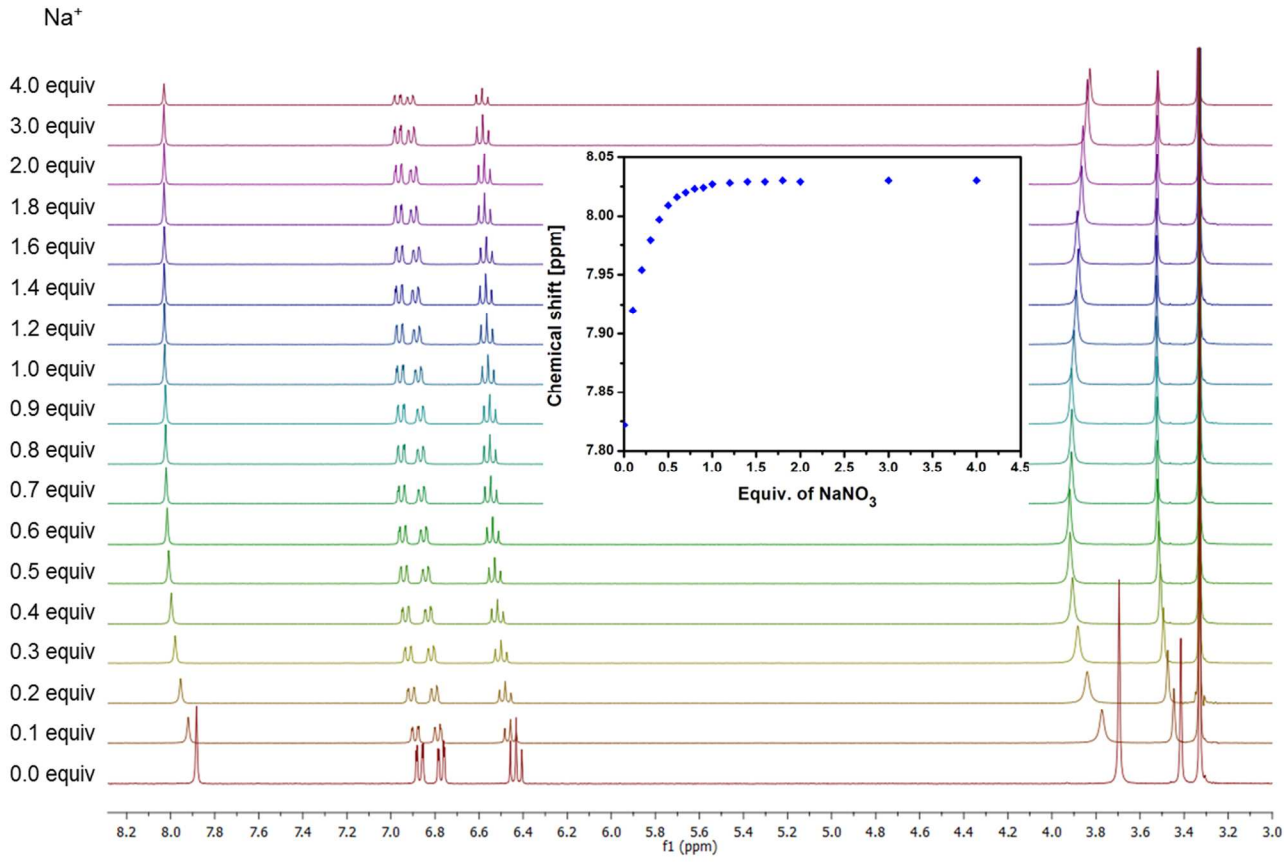

Figure S13: ^{1}H NMR spectral changes of the metallohost LNi (400 MHz, DMSO-d_6, 0.02 M) upon the addition of $NaNO_3$ in deuterated DMSO.

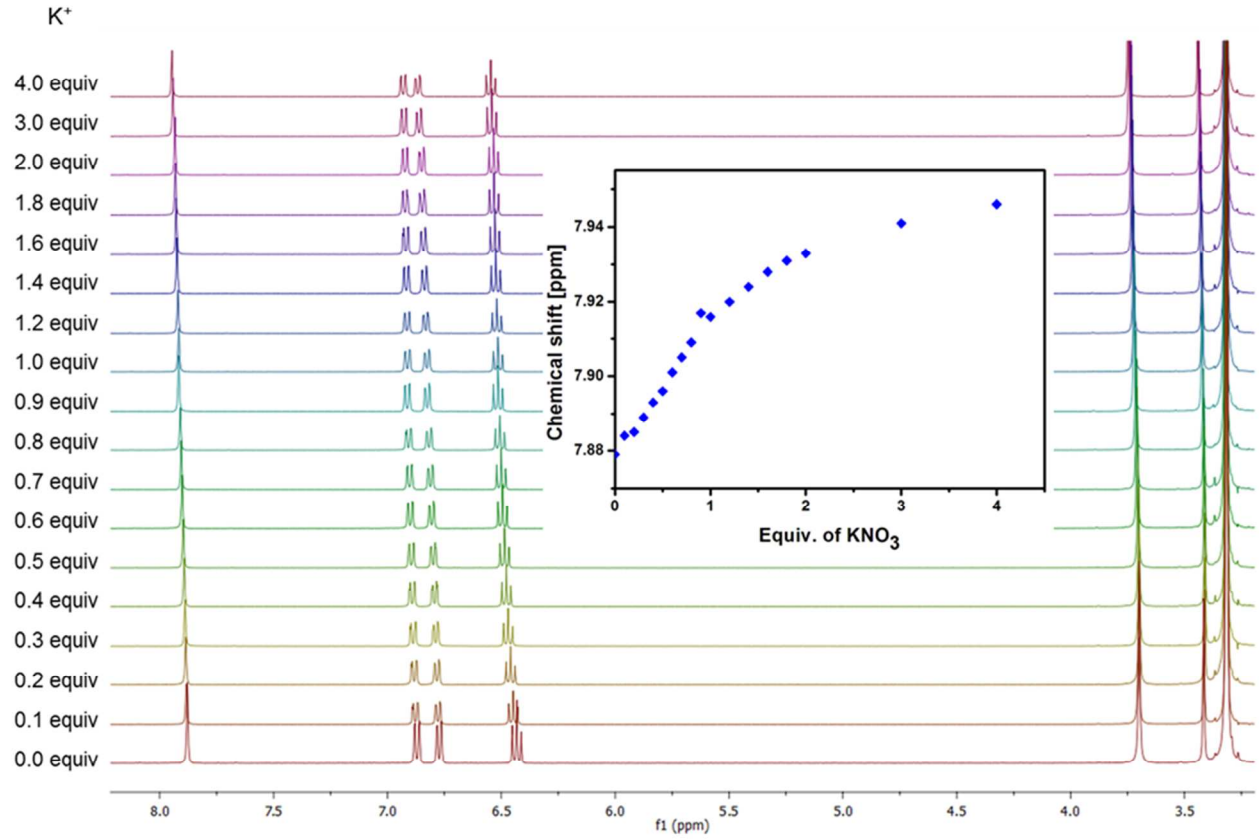

Figure S14 : ^{1}H NMR spectral changes of the metallohost LNi (400 MHz, DMSO-d_6, 0.02 M) upon the addition of KNO_3 in deuterated DMSO.

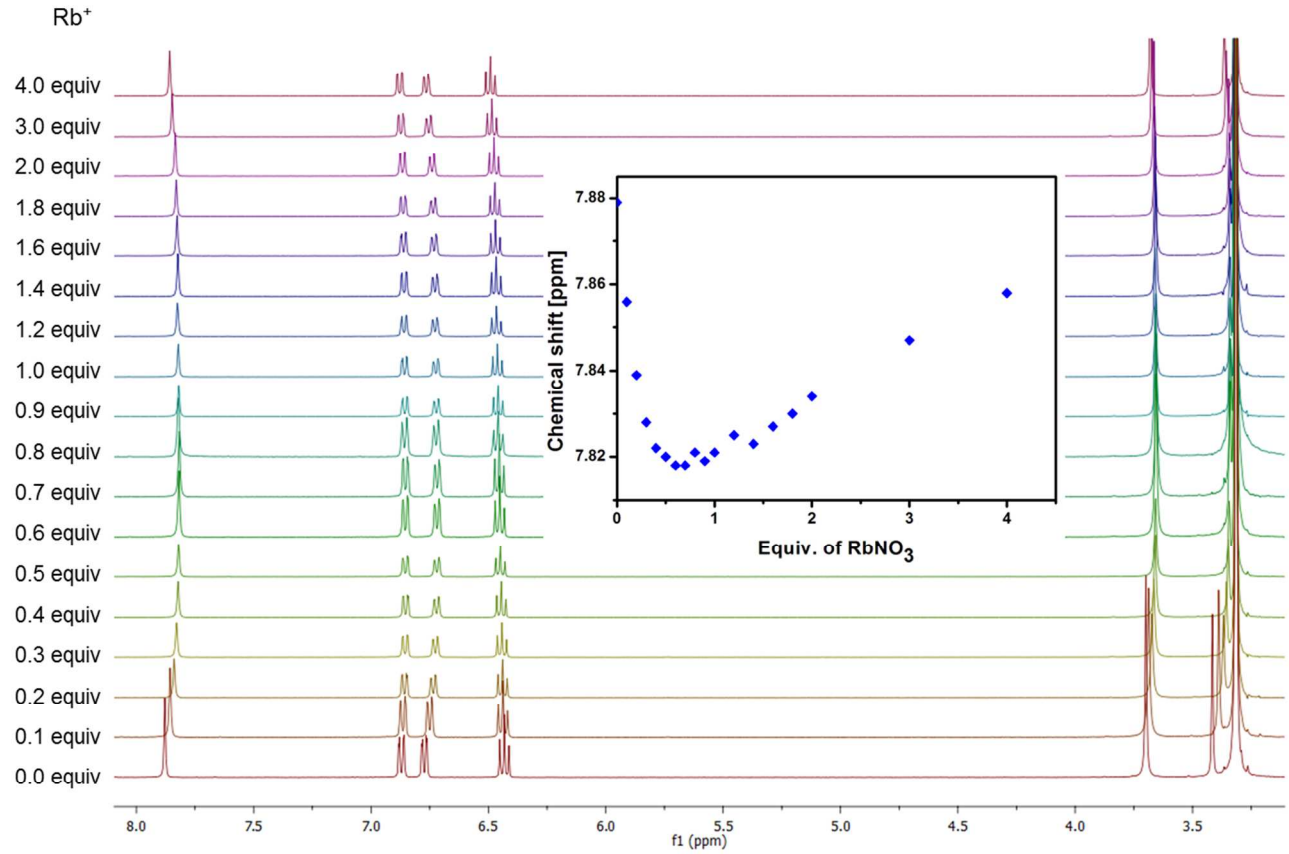

Figure S15 : ^{1}H NMR spectral changes of the metallohost LNi (400 MHz, DMSO-d_6, 0.02 M) upon the addition of $RbNO_3$ in deuterated DMSO.

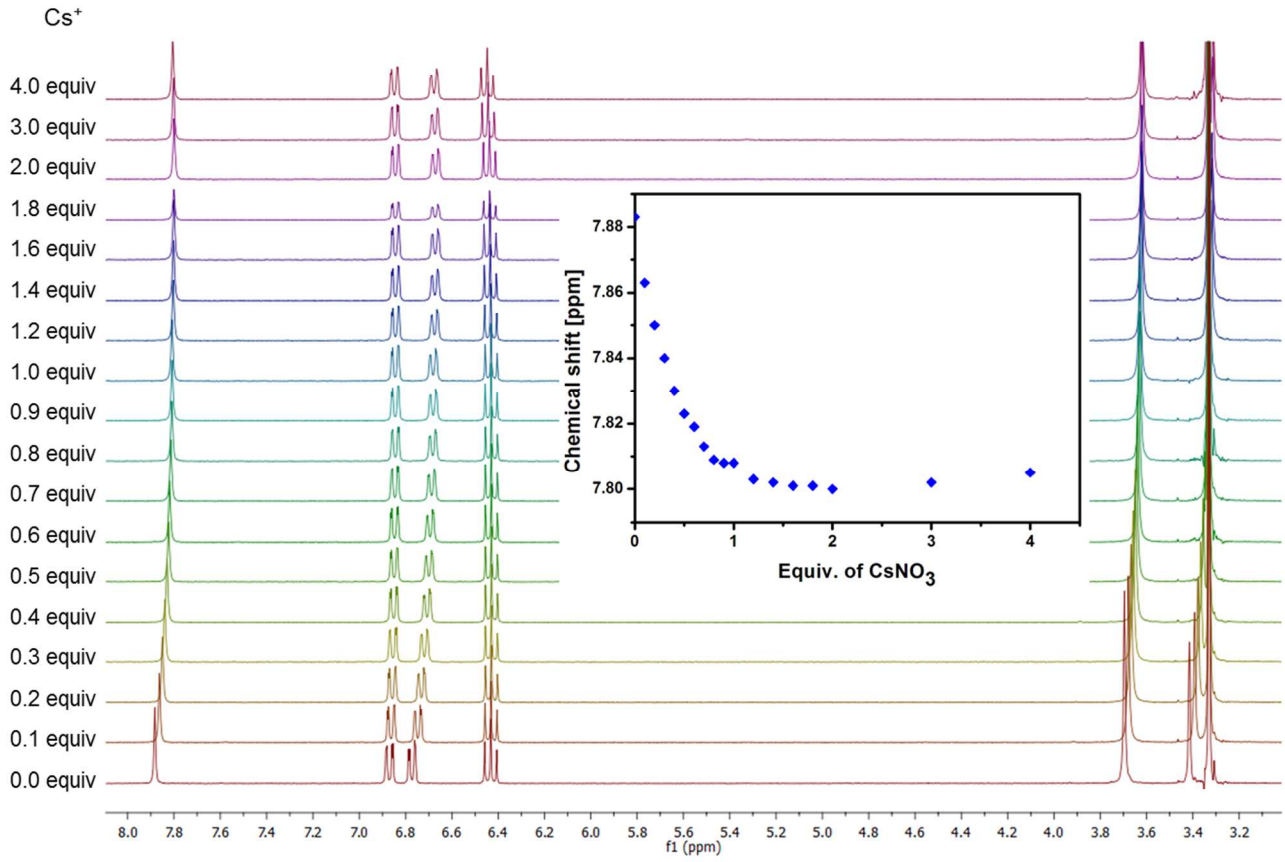

Figure S16 : ^{1}H NMR spectral changes of the metallohost LNi (400 MHz, DMSO-d_6, 0.02 M) upon the addition of $CsNO_3$ in deuterated DMSO.

XPRD Diffractograms of the alkali metal complexes

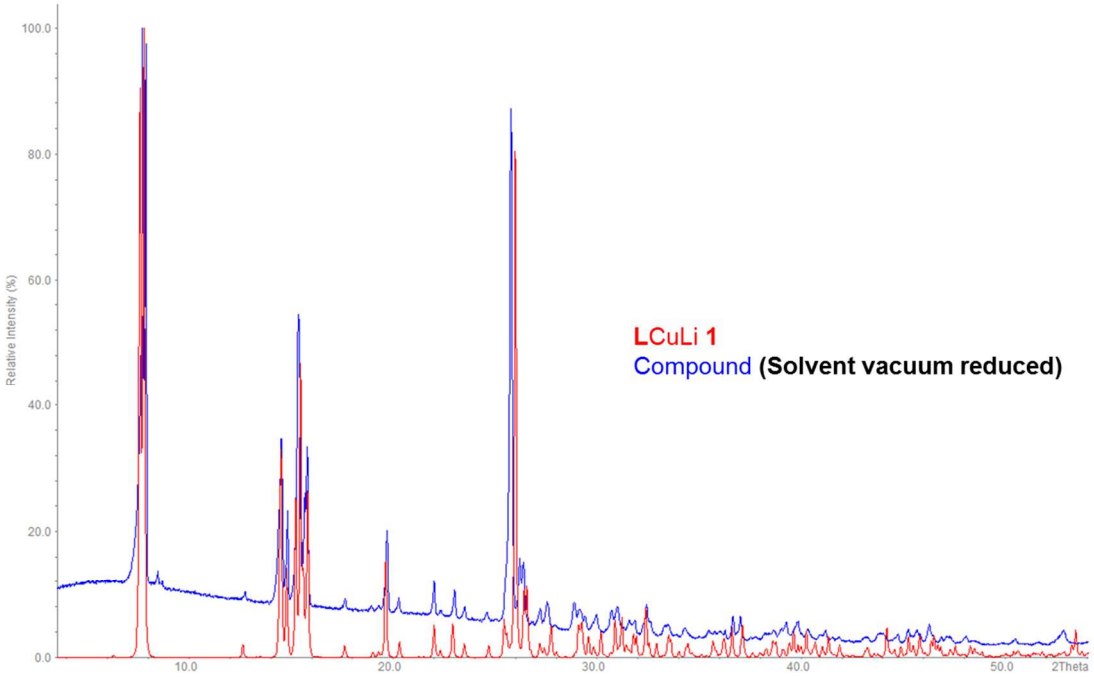

Figure S17 : XPRD diffractogram of the LCuLi (1) compounds obtained by removing the solvent under vacuum compared with the crystal structure simulation 1.

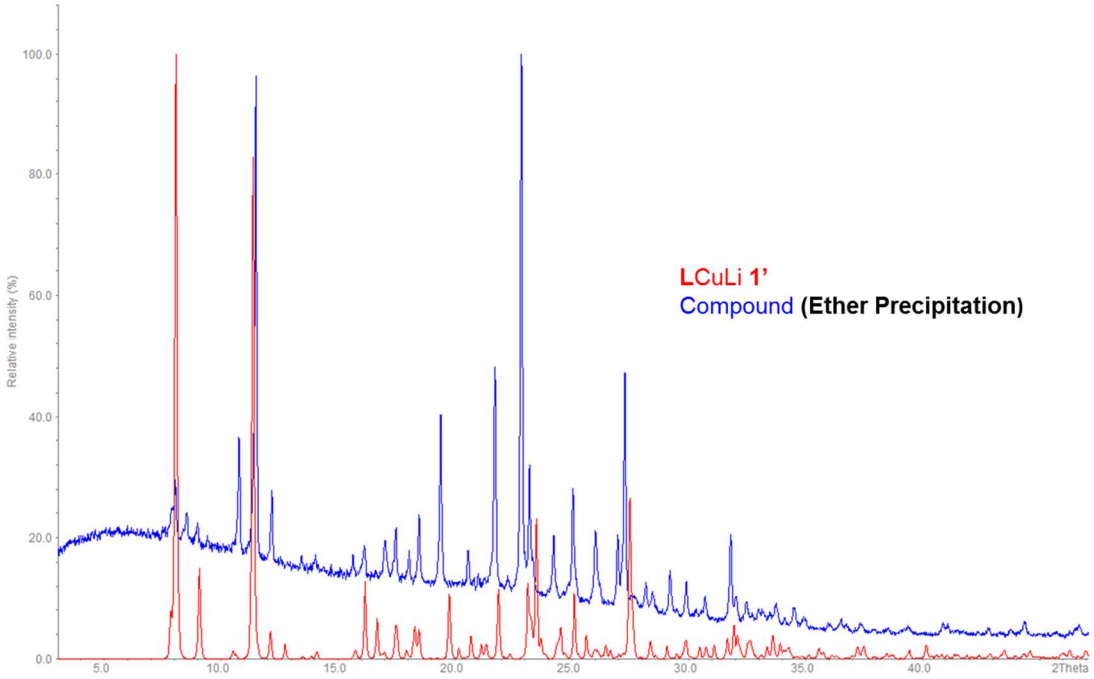

Figure S18 : XPRD diffractogram of the LCuLi (1') compounds obtained by ether precipitation compared with the crystal structure simulation 1'.

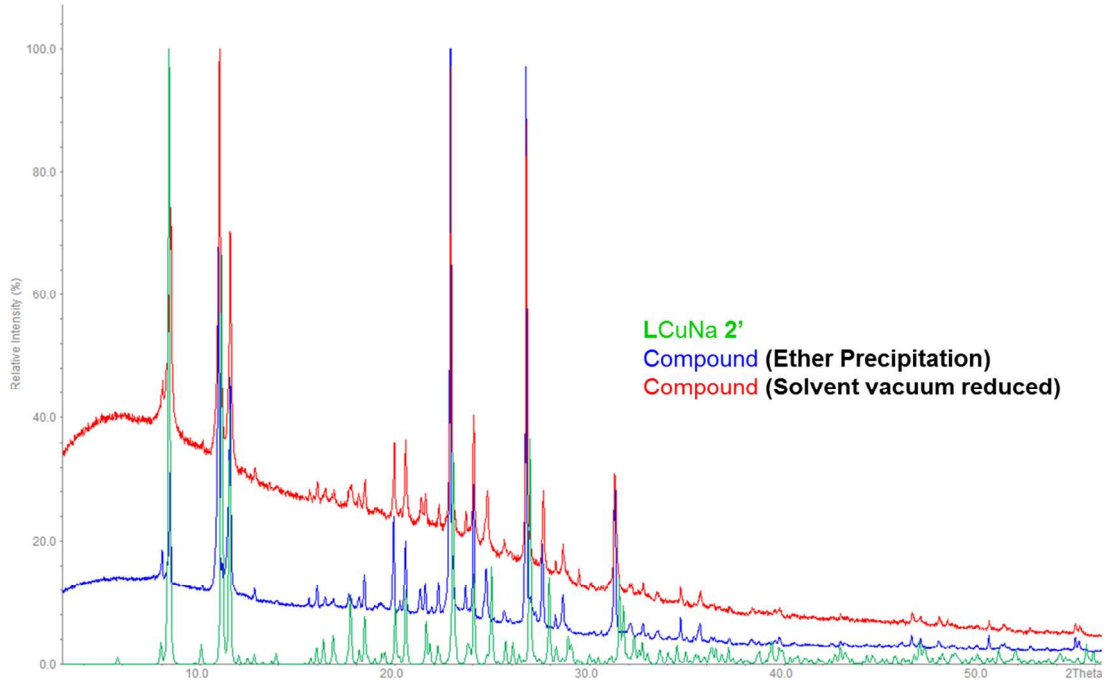

Figure S19 : XPRD diffractogram of the LCuNa (2') compounds obtained by removing the solvent under vacuum and ether precipitation compared with the crystal structure simulation 2'.

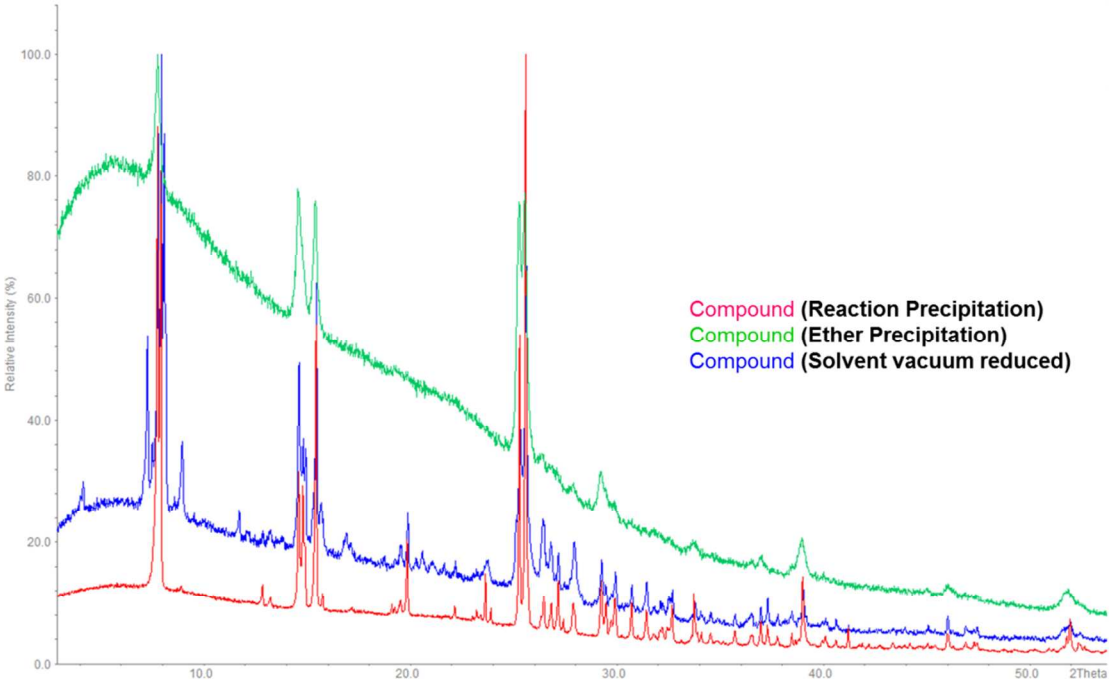

Figure S20 : XPRD diffractogram of the LCuK (3) compounds obtained by removing the solvent under vacuum and ether precipitation compared with the crystal structure simulation 3.

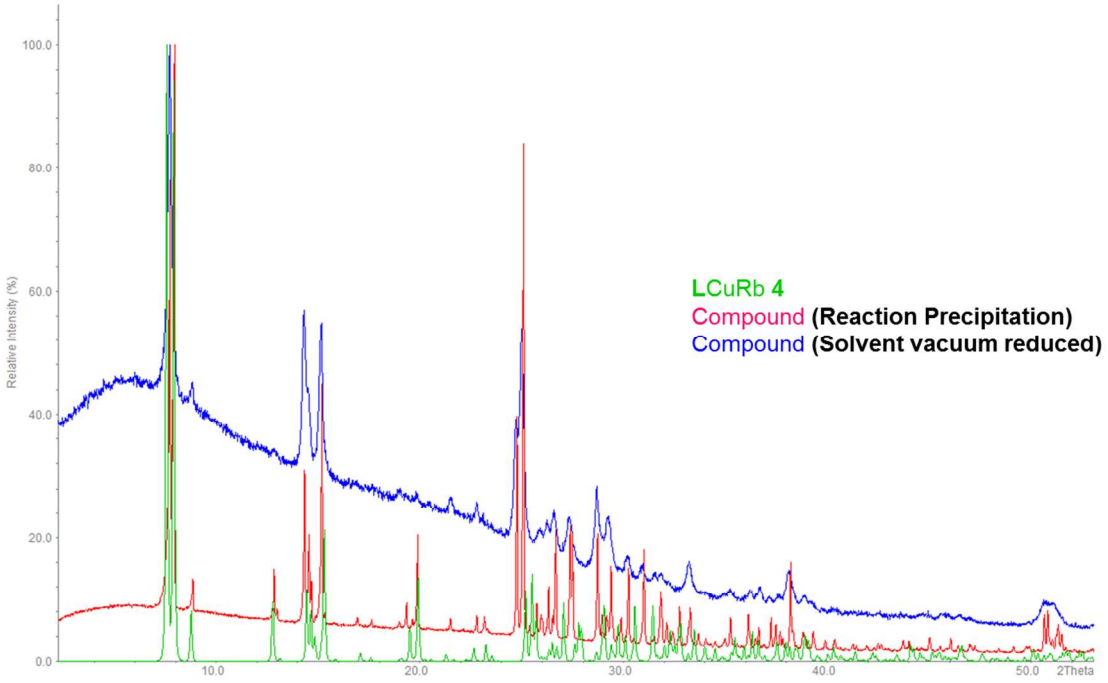

Figure S21: XPRD diffractogram of the LCuRb (4) compounds obtained by removing the solvent under vacuum, ether precipitation and the precipitation resulting of the reaction compared with the crystal structure simulation 4.

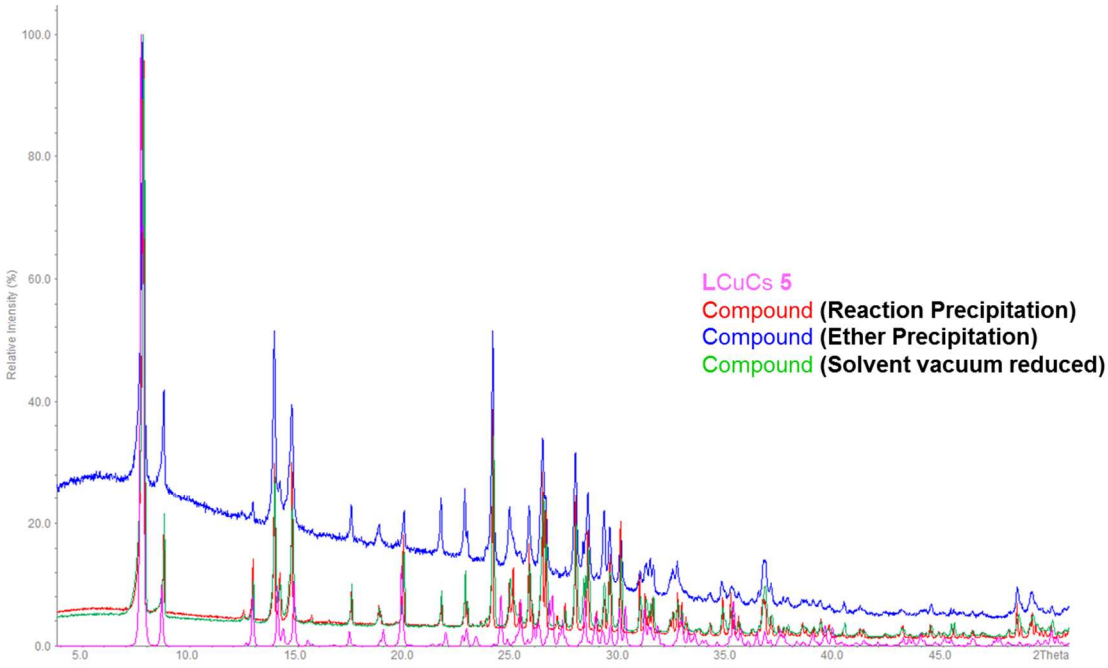

Figure S22: XPRD diffractogram of the LCuCs (5) compounds obtained by removing the solvent under vacuum, ether precipitation and the precipitation resulting of the reaction compared with the crystal structure simulation 5.

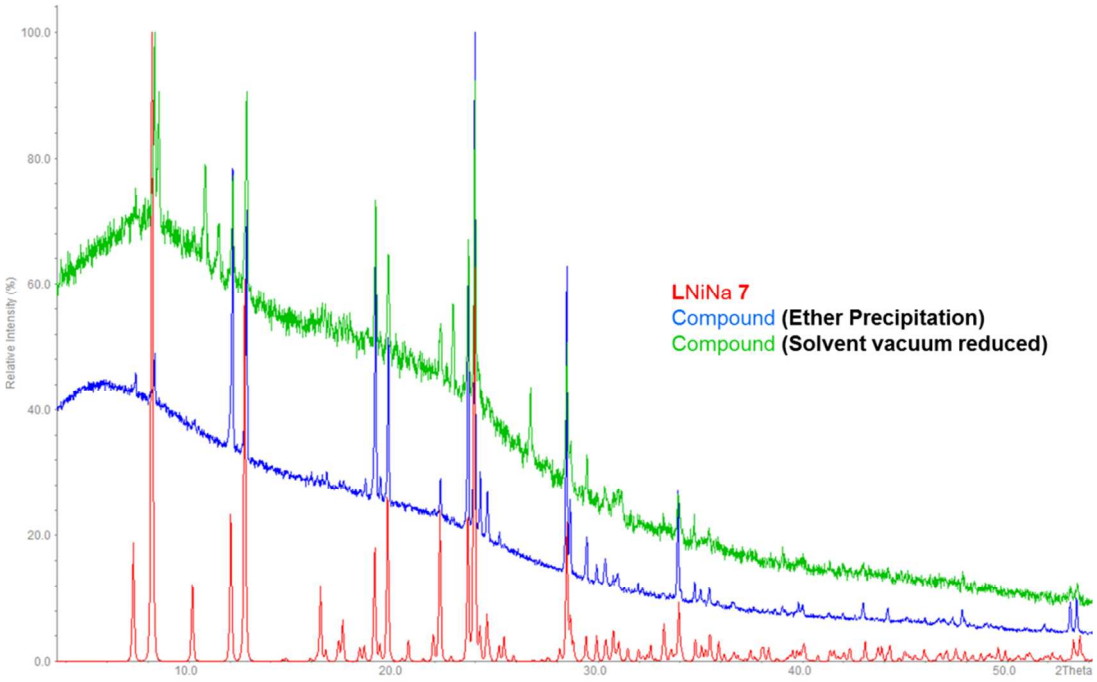

Figure S23 : XPRD diffractogram of the LNiNa (7) compound obtained by ether precipitation compared with the simulation of the crystal structure 7.

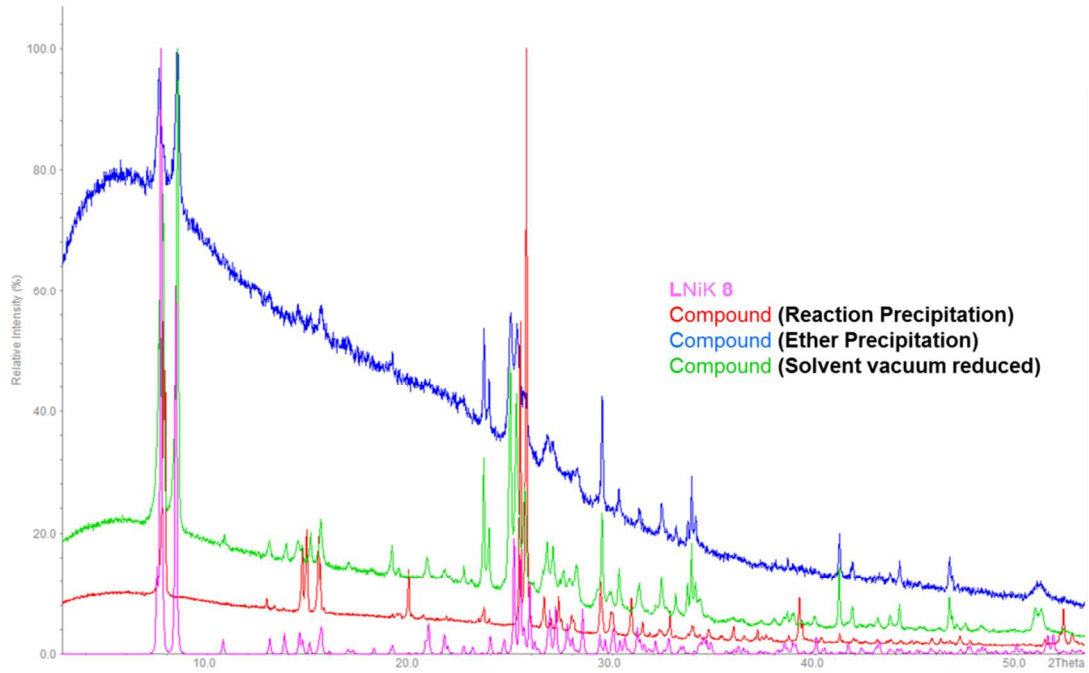

Figure S24 : XPRD diffractogram of the LNiK (8) compound obtained by ether precipitation compared with the simulation of the crystal structure 8.

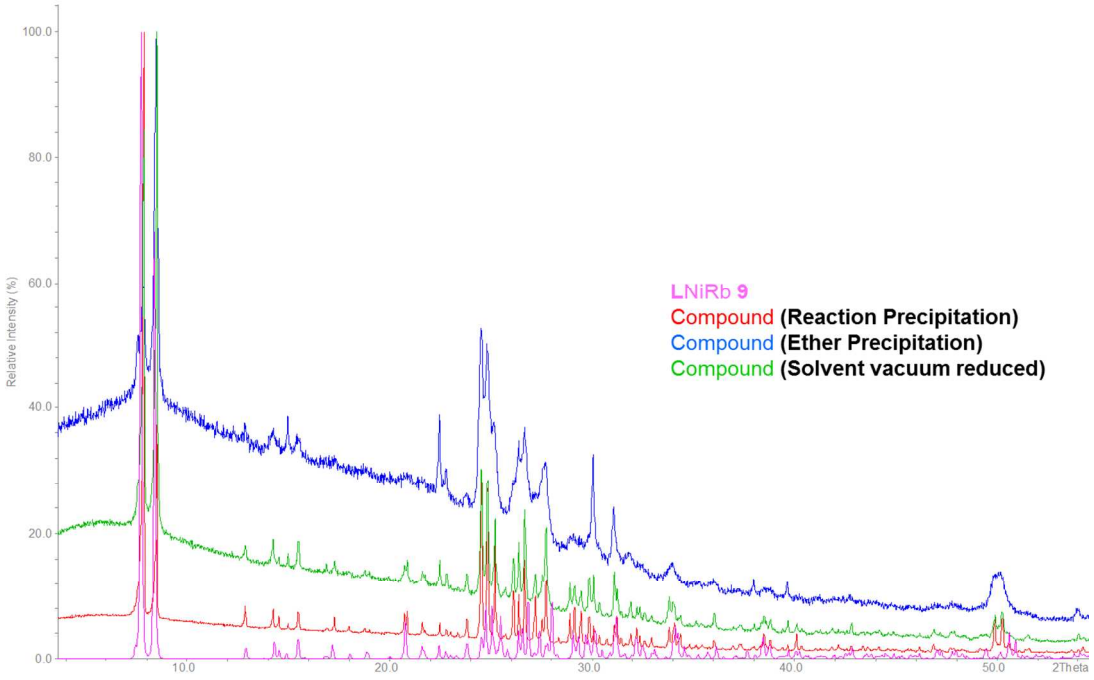

Figure S25 : XPRD diffractogram of the LNiRb (9) compound obtained by ether precipitation compared with the simulation of the crystal structure 9.

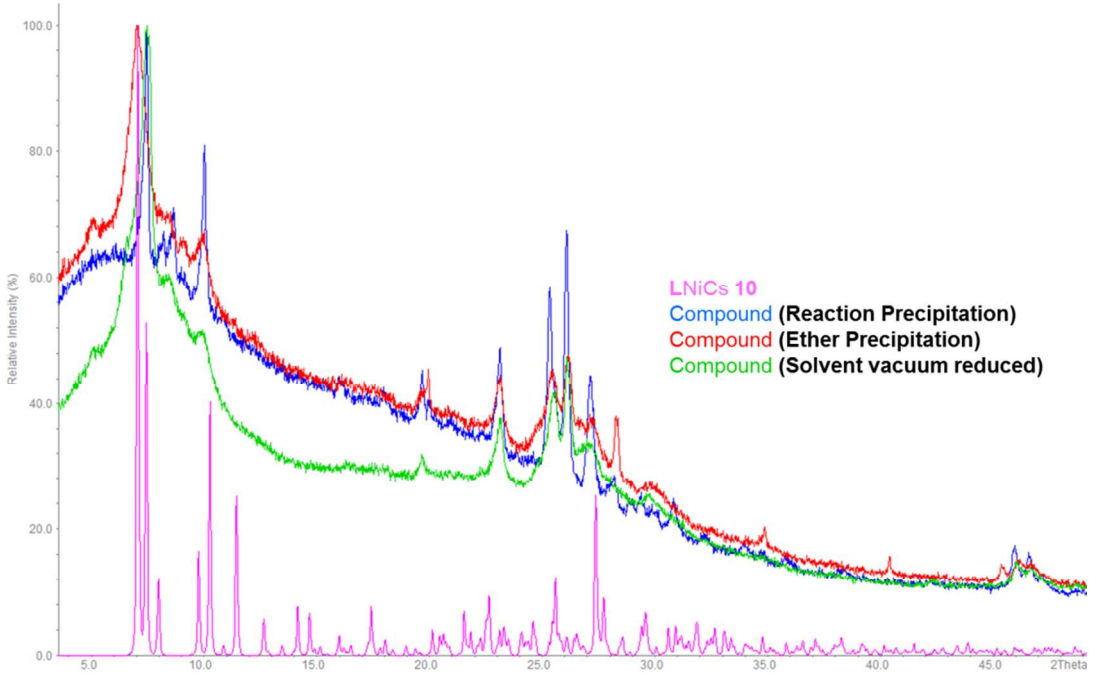

Figure S26: XPRD diffractogram of the LNiCs (10) compound obtained by ether precipitation compared with the simulation of the crystal structure 10.

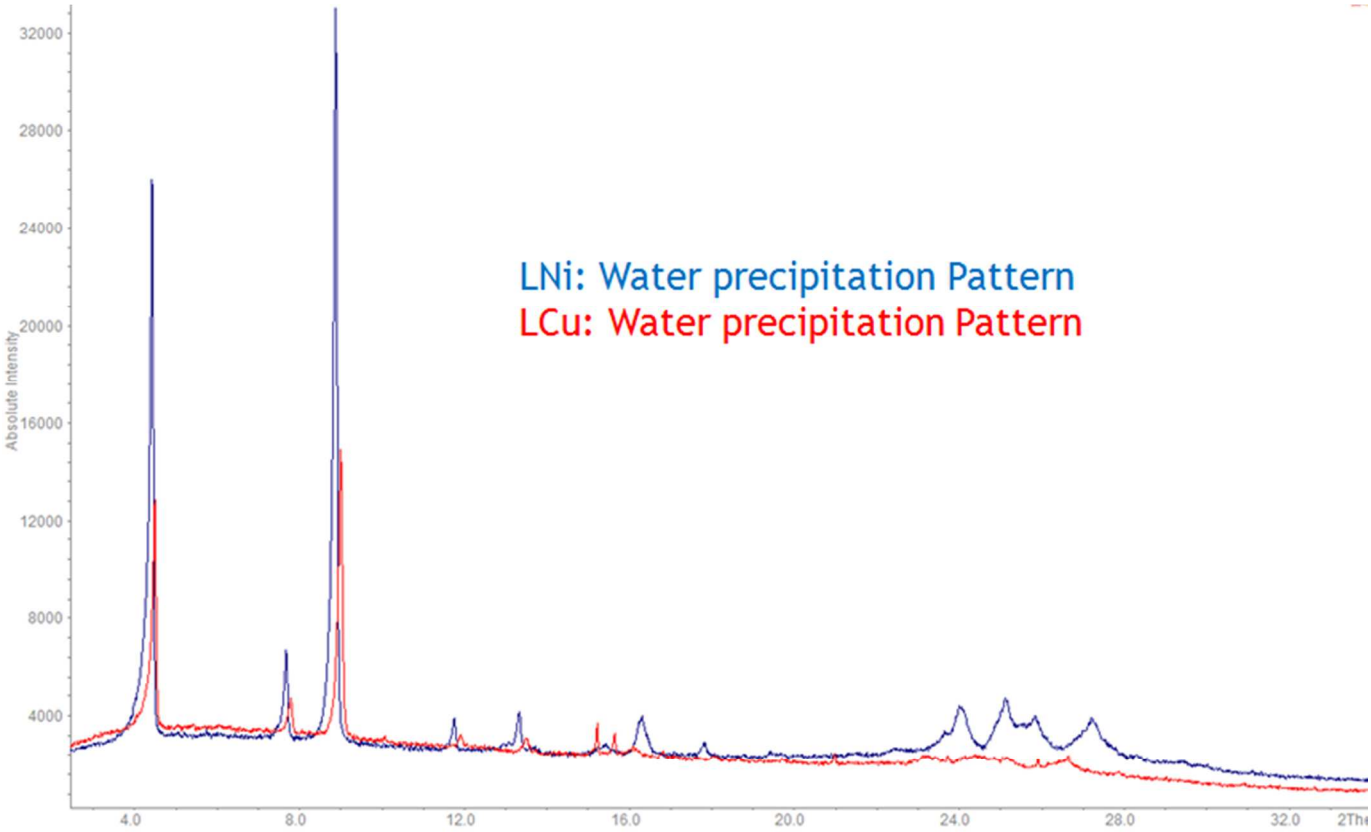

Figure S27 : XPRD diffractogram of the new compound based on LNi and LCu obtained by precipitation in water from a solution made of the correspondent LM1 in DMSO.

Mass spectrum of the complexes 1-10.

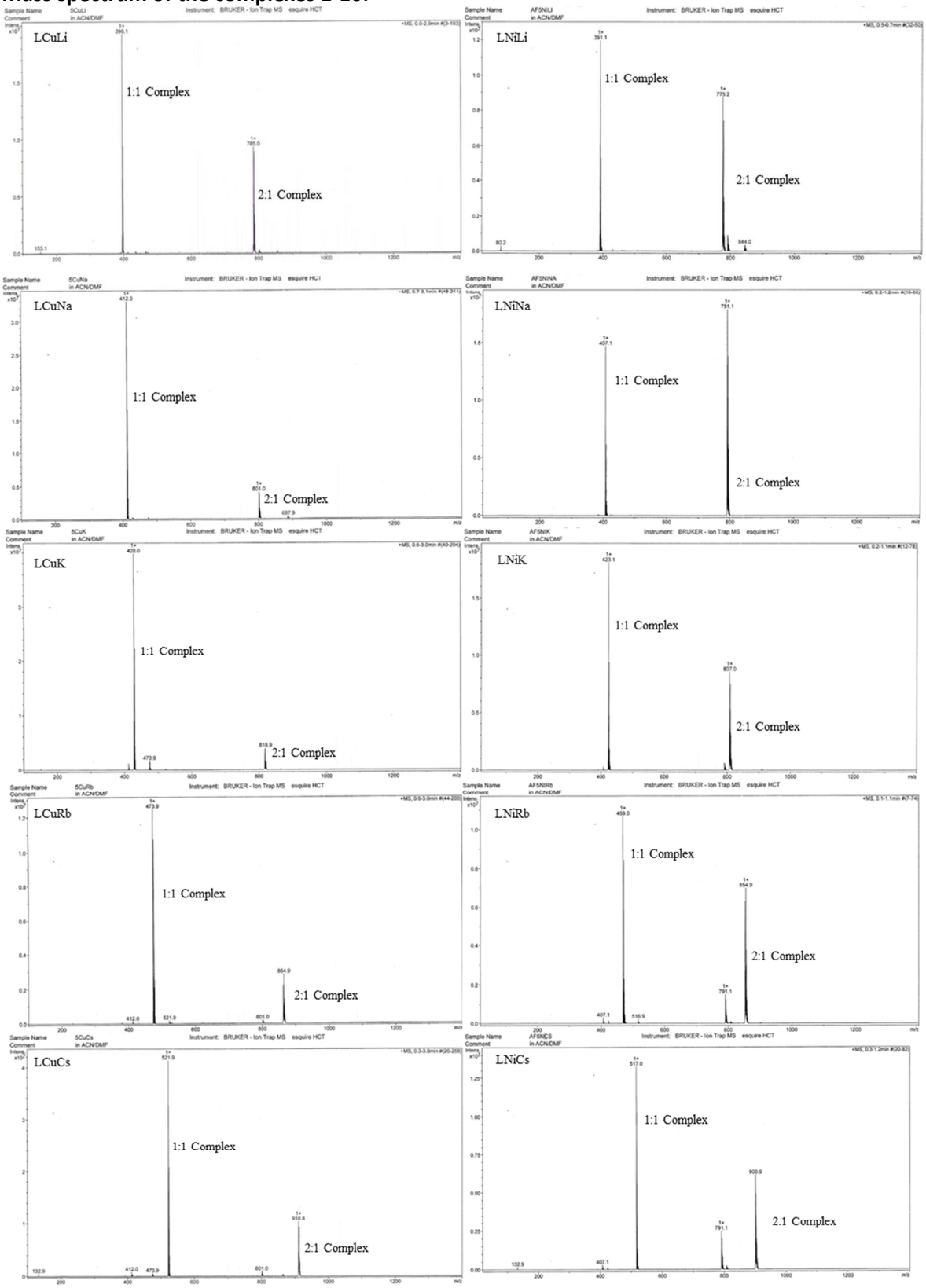

Figure S28: Mass spectrum of the Cu- (1-5) and Ni-Complexes (6-10).

Crystallography

CuLi (1)

[{LCuLi(μ-NO_3)(μ-H_2O)}$_2$]$_n$. The compound **LCuLi (1)** is obtained as green rod-shaped single crystals by slow vapor diffusion of Et_2O into a ACN/EtOH mixture containing **1** after reacting **H_2L** first with $Cu(OAc)_2$, then adding $LiNO_3$. It crystallizes in the triclinic space group *P*-1 (No. 2) in a 1:1:1 stoichiometry for L:Cu:Li. Two non-equivalent entities are present in the asymmetric unit L1:Cu1:Li1 and L2:Cu2:Li2. The transition metal ion is coordinated in an octahedral fashion with a perfect square planar base formed by the N_2O_2 chelating moiety of the ligand with Cu–O distances of 1.930(2) and 1.917(2) Å for O2 and O3 coordinating to Cu1, respectively 1.905(2) and 1.938(2) Å for O6 and O7 binding to Cu2 of the phenolate moieties and Cu–N distances of 1.950(2) and 1.943(2) Å for N1 and N2 (Cu1), respectively, 1.844(2) and 1.843(2) Å for N3 and N4 (Cu2) of the imine groups. The angle sum around the copper ions sum up to 360.08° for Cu1 and 359.88° for Cu2, indicating the planarity of the coordination. The coordination of the copper ions is completed by two oxygen atoms of two different nitrates moieties with axial Cu1−O distances of 2.683(2) Å for O9 and 2.637(2) Å for O10, and the axial Cu2−O distances of 2.682(2) Å for O12 and 2.687(2) Å for O14. The presence of a Jahn-Teller effect led to this elongated tetragonal distortion. The lithium ion is only coordinated to one side of the ligand via O3 and O4 with 2.073(4) and 2.031(4) Å distances respectively for Li1 and via O7 and O8 with 2.049(4) and 2.086(4) Å distances for Li2. Their tetrahedral coordination sphere is completed by O12 (Li1) and O9 (Li1) of a nitrate anion with 2.214(5) Å and 2.206(5) respectively, and a water molecule which binds via O15 to Li1 and O16 to Li2 at 1.968(5) Å and 1.967(5) Å, respectively. This latter water molecule acts as bridging ligand towards a lithium ion of the next neighbor complex with a Li1'-O16 distance of 1.980(5) Å and of 1.986(5) Å for Li2'–O15. It is surprising that the negatively charged nitrate anion forms the longer Li–O bond compared to the neutral and bridging water molecule. This might be due to the hydrogen bonding system with can be observed by short O–O distances between O10 and O15 as well as O15 and O2, O15 and O5 and O15 and O6. Hence, the hydrogen atoms of the water molecule O15 are likely involved in hydrogen bonds between these oxygen atoms, and it is envisageable to alternatively form HNO_3 and ^-OH as ligands on the lithium cation. The distance between the lithium ion and the mean plane formed by the Cu(II) ion and the N_2O_2 entity is 0.272 Å for Cu1 or 0.195 Å for Cu2 and shows that the alkali metal ion is out of plane compared to the **LCu**-complex.
Since the oxygen atoms O15 and O16 act as bridging atoms between the lithium ions of neighbor complexes, and the nitrate anions acting as bridging ligands towards the Cu(II)- as well as the water molecule, an overall one-dimensional (1D) coordination polymer is obtained, in which the ligand molecules are arranged alternatingly along the crystallographic *c*-axis. This arrangement can also be described as one-dimensional Li-water-Li-water-chains surrounded by two one-dimensional Cu-nitrate-water-chains. The distance between neighbor lithium ions within the coordination polymer is then 3.503(6) Å (Li1–Li2) and 3.484(6) (Li2#1–Li1)

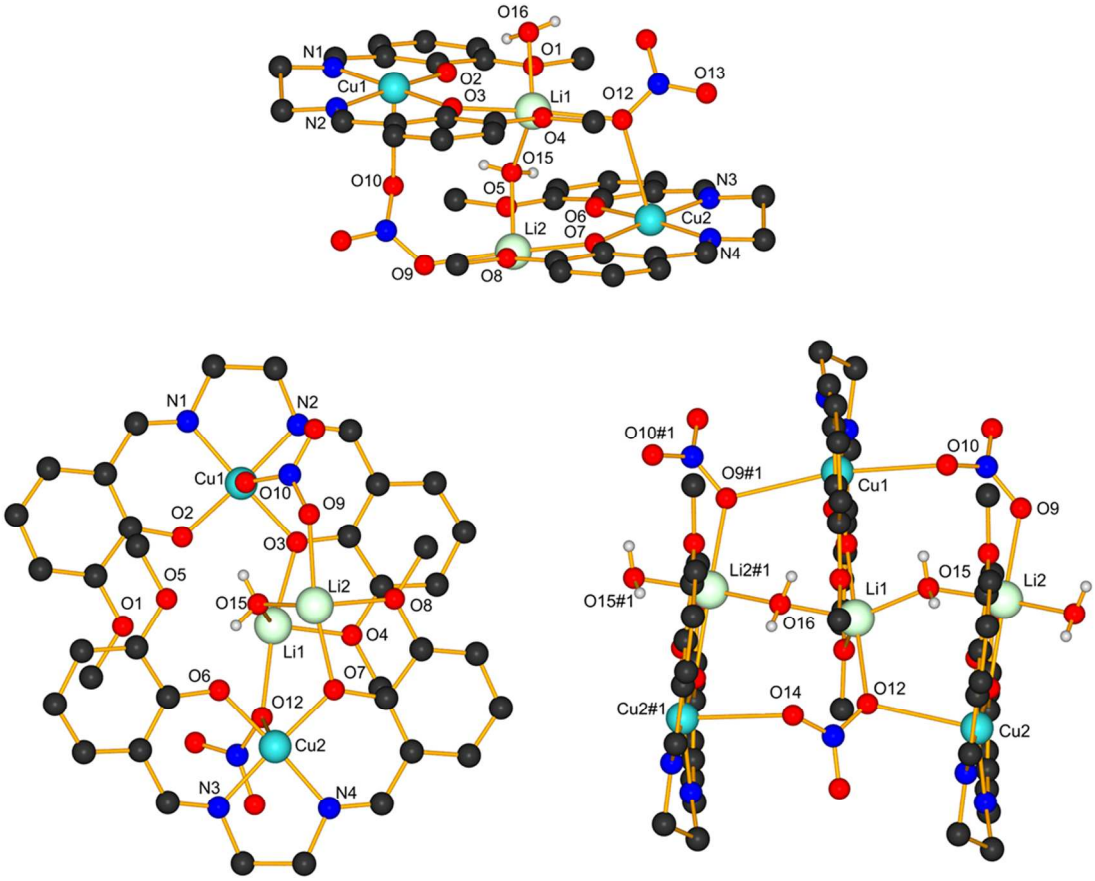

Figure S29 : Crystal structure of LCuLi complex 1 showing the connection into a 1D-structure. Partial H-atoms were omitted for clarity.

LCuLi (6)

[(LNiLi(NO_3))$_2$(μ-H_2O)]. Suitable crystals of the **LNiLi** complex (**6)** with the nickel (II) ion coordinated as M_1 in the imine-based N_2O_2 site have been obtained as orange block-like crystals by slow vapor diffusion of Et_2O into an ACN/EtOH solution containing **H_2L** with Ni(OAc)$_2$ and $LiNO_3$. In contrast to **1**, the compound crystallizes in an orthorhombic *P*bca space group (No. 61) in a 1:1:1 stoichiometry for L:Ni:Li. Like for **1**, two non-equivalent entities are present in the unit cell as L1:Ni1:Li1 and L2:Ni2:Li2. The transition metal ion is coordinated in a square planar fashion by the N_2O_2 chelating moiety of the ligand with Ni–O distances of 1.844(2) and 1.838(2) Å for O2 and O3 (Ni1), 1.842(2) and 1.852(2) Å for O6 and O7 (Ni2) of the phenolate moieties and Ni–N distances of 1.835(2) and 1.840(2) Å for N1 and N2 (Ni1), respectively, 1.844(2) and 1.843(2) Å for N3 and N4 (Ni2) of the imine groups. The angle sums around the nickel ions are 360°(Ni1) and 360.02°(Ni2), indicating the better planarity of the coordination for Ni(II) than for Cu(II). In contrast to **1**, the cavity formed by the O_2O_2 coordination site is now centrally occupied by a lithium ion, linking only the two phenolate oxygen atoms O2 and O3 for Li1 or O6 and O7 for Li2 with Li-O distances 1.984(7) Å and 2.010(7) Å, respectively 1.989(5) Å and 2.041(7) Å. O1 and O4 are weakly coordinated to Li1 with 2.570(7) and 2.605(7), and so are O5 and O8 for Li2 with 2.542(7) and 2.677(6). The distance between the lithium ion and the mean plane formed by the Ni(II) ion and the N_2O_2 is 0.043 Å for Ni1 or 0.021 Å for Ni2 and shows that the alkali metal ion is practically in plane with **LNi**. Further coordination to the lithium ions occurs via O9 (Li1) and O13 (Li2) of nitrate ions with distances of

2.032(7) Å and 1.990(7) Å respectively and a bridging water molecule O12 between the two alkali metal ions with distances of 2.006(7) Å (Li1) and 2.009(6) Å (Li2). In contrast to **1**, no one-dimensional chain is formed by bridging water molecules. Instead, a short contact between the Ni(II) and the π-system of the neighbor complex allows an expansion along the *a*-axis. The distance between neighbor lithium ions within the sequence is then 3.403(9) Å (Li1–Li2). While the pairs pack along the a-direction, edge to face C–H…π interactions shorter than 2.9 Å between next neighbor chains are observed between e.g. H32 of one ligand and the aromatic ring C20-C25 of the next ligand in a parallel chain.

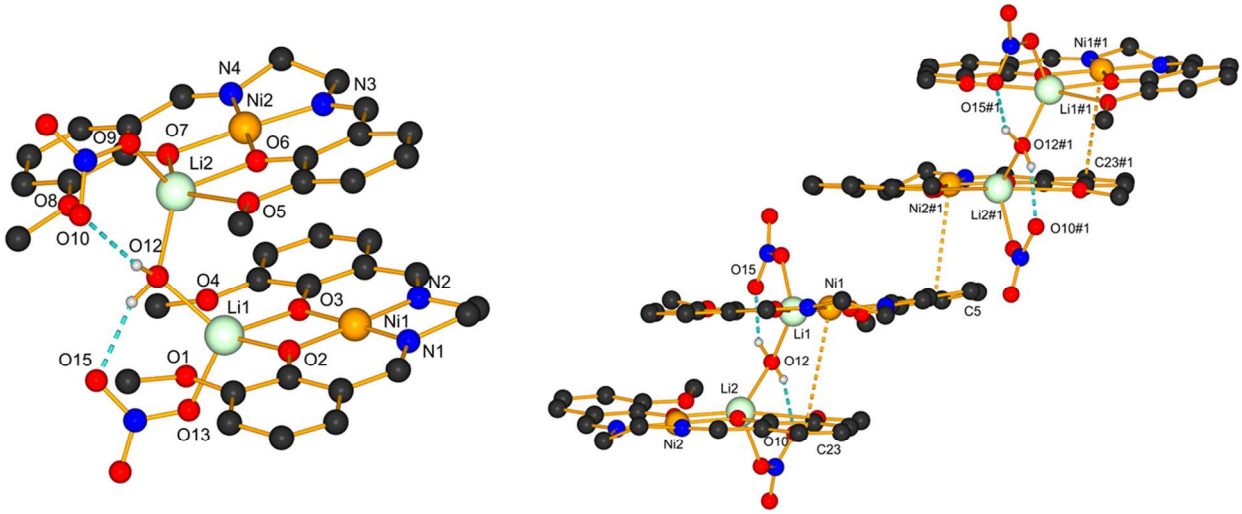

Figure S30 : Crystal structure of LNiLi complex 6 showing the connection into a 1D-structure. Partial H atoms were omitted for clarity.

LCuNa (2)

[LCuNa(NO$_3$)]$_n$. Single crystals of **LCuNa** are obtained as orange needles by slow evaporation of an ACN/EtOH solution of **LCuNa** after reacting **H$_2$L** first with Cu(OAc)$_2$, then adding NaNO$_3$. Compound **2** crystallizes in the monoclinic space group $P2_12_12_1$ (No.19) in a 1:1:1 stoichiometry for L:Cu:Na and with a single moiety in the asymmetric unit. As for **1** the transition metal ion is coordinated in a quasi-square planar fashion by the N_2O_2 chelating moiety of the ligand with Cu–O distances of 1.915(2) Å for O2 and 1.928(2) Å for O3 of the phenolate moieties and Cu–N distances of 1.948(2) Å and 1.941(2) Å for N1 and N2, respectively, of the imine groups and an angle sum of 360.08°. The coordination of the copper ion can also be interpreted as square pyramidal if the Cu1–O7#5 contact with a distance of 3.072(4) Å is considered as a weak bond due to its positive but weak contribution of 0.021 to the bond valence. The second coordination site, O_2O_2, is occupied by the sodium ion involving the phenolate oxygen atoms O2 and O3 with Na-O distances of 2.383(4) Å and 2.306(4) Å as well as the methoxide groups O1 and O4 with Na-–O distances of 2.723(4) Å and 2.552(4) Å respectively. The distance between the sodium ion and the mean plane formed by the Cu(II) ion and the N_2O_2 is 0.156 Å and shows that the alkali metal ion is slightly out of plane. Its hexacoordinated ligand sphere is completed by O5 and O6 of a nitrate ion with 2.460(4) Å and 2.421(4) Å, respectively.
Interestingly, and only for the structures containing sodium as M_2, there is a short contact between Na(I) and C4 of a neighboring π-system with 2.900(5) Å, inducing a bending of the corresponding aromatic ring

of 15.38° out of the plane formed by the Cu-N_2O_2-entity **(Table S1)** and resulting in non-planarity of the ligand. While the Na-π contact allows an expansion of the structure into the direction of the *a*-axis, a growth along the *c*-axis is revealed by the short contact with Cu1 belonging to the N_2O_2 site and O7 of the nitrate ion.

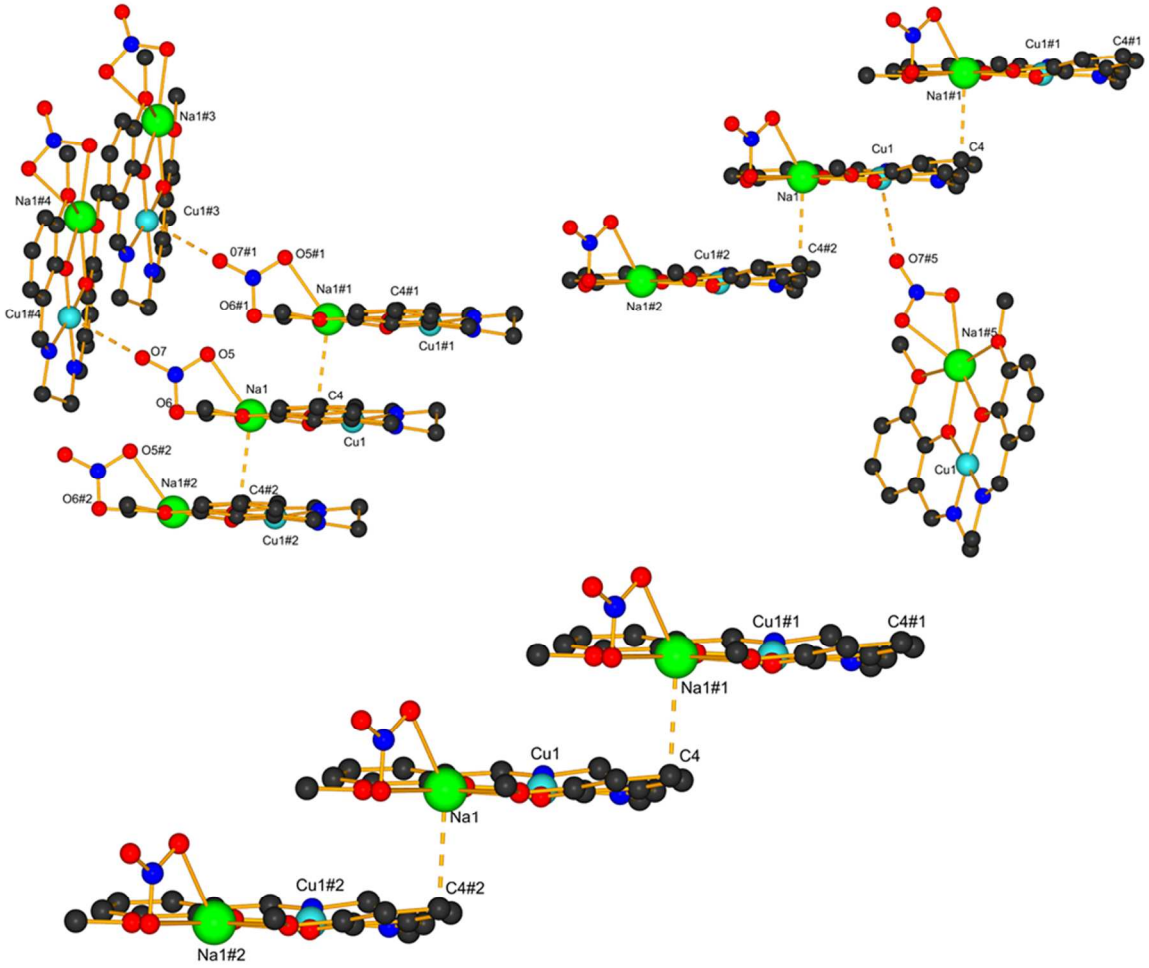

Figure S31 : Solid state structure of LCuNa complex 2 connectivity between the complexes. All H-atoms were been omitted for more clarity.

LNiNa (7)

[LNiNa$(NO)_3$]. A similar structure than for **2** is obtained under analogous conditions with Ni(II) as M1 coordinated in the imine-based N_2O_2 site. In contrast to **2**, the compound crystallizes in the monoclinic space group $P2_1/c$ (No.14) with one 1:1:1 complex per asymmetric unit. Again, the Ni(II) is coordinated in a perfectly square planar fashion with Ni–O distances of 1.843(3) for O2 and 1.845(3) Å for O3 of the phenolate moieties and Ni–N distances of 1.841(4) and 1.843(3) Å for N1 and N2 of the imine groups. The sodium ion in the O_2O_2 cavity is bound by the phenolate oxygen atoms O2 and O3 with distances of 2.360(3) Å and 2.369(3) Å as well as by the methoxide O1 and O4 oxygen atoms with 2.546(3) Å and 2.550(3) Å. The nitrate oxygen atoms O5 and O6 complete the coordination sphere of the alkali metal ion

with 2.458(4) Å and 2.518(3) Å, respectively. An expansion along the *a*-axis is again produced by a weak contact between Na(I) and the neighbor π-system with 3.093 Å, leading to a slight distortion of one aromatic ring out of the ligand plane, which is less important than in the **LCuNa** complex **(Table S1).** The distance between the sodium ion and the mean plane formed by the Ni(II) ion and the N_2O_2 is 0.221 Å showing that the alkali metal ion is more out of plane than in compound **2**.

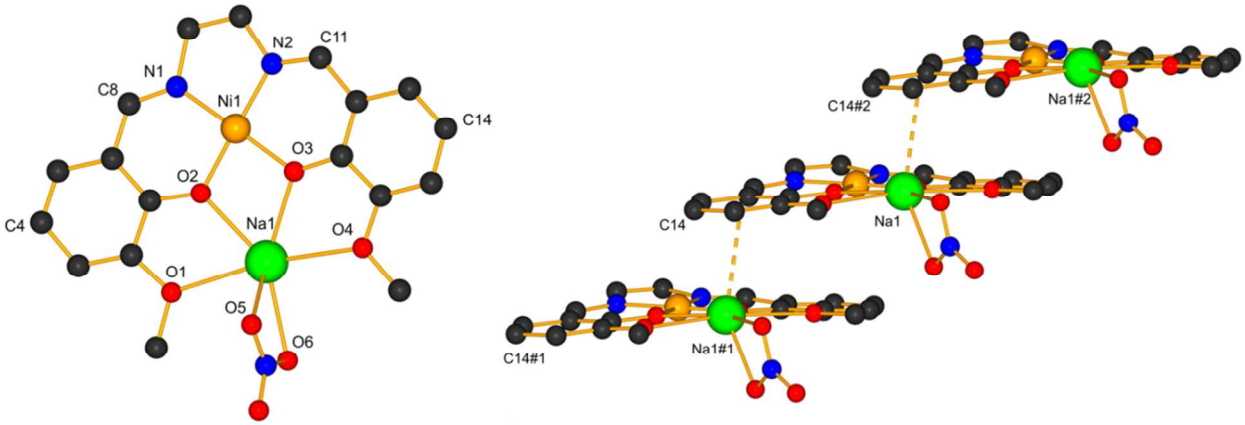

Figure S32 : Asymmetric of LNiNa complex 7 (left) and its arrangement along the *a*-axis (right). All H-atoms were been omitted for more clarity.

LNiK (8)

[(LNiK(μ-NO_3)]$_n$. While we were unable to obtain single crystals of the corresponding Cu-complex "[LCuK(NO_3)]" **(3)**, single crystals of complex **LNiK (8)** are formed as orange needles by slow evaporation of an ACN/EtOH solution of **LNiK** after reacting **H_2L** previously with Ni($OAc)_2$, then adding KNO_3. As compound **7**, **8** crystallizes in the monoclinic space group $P2_1/c$ (No.14) and features a 1:1:1 complex of L:Ni:K in the asymmetric unit. The Ni(II) ion is again coordinated in a square planar fashion by the N_2O_2 moiety of the ligand with Ni–O distances of 1.847(2) for O2 and 1.852(2) Å for O3 of the phenolate moieties and Ni–N distances of 1.842(3) and 1.839(2) Å for N1 and N2, respectively, of the imine groups and an angle sum of 360.06°.The potassium ion is coordinated by all four oxygen atoms of the O_2O_2 site. As the potassium ion is too big to fit into the cavity formed by the O_2O_2 coordination site, the cation is entirely out of the ligand plane and adopts a pentagonal antiprismatic coordination involving the four oxygen atoms of the O_2O_2 moiety of one ligand, the O_2O_2 moiety of a next neighbor ligand as well as two oxygen atoms of two bridging nitrate ions. The shortest bonds are formed with the bridging nitrate oxygen atoms O5 and O5' with 2.760(3) and 2.740(3) Å, respectively, with the methoxide oxygen atoms O1 and O4#1 with K-O distances of 3.071(3) and 2.887(2) Å as well as phenolate with the oxygen atoms O2, O3, O2#1, O3#1 with the K-O distances of 2.917(2), 2.919(2), 2.936(2) and 3.055(3) Å. The contacts of the potassium ion with the methoxide oxygen atoms O4 and O1#1 are not contributing significantly to the bond valence law. The bridging of the potassium ion between two ligands and the bridging nitrate anions between the potassium ions along the same *c*-axis lead to the formation of a one-dimensional (1D) coordination polymer.
The distances between the potassium ion and the mean plane formed by the Ni(II) ion and the N_2O_2 moiety are 0.875 Å to one side and 1.675 Å to the other side of a Ni-complex. The distance between neighbor potassium ions within the sequence is then 3.558(1) Å, while it is 3.558(1) Å for the two next Ni(II) ions. The offset rotation angle between the two neighbor ligands, leading to the antiprismatic coordination, is 46.08°.

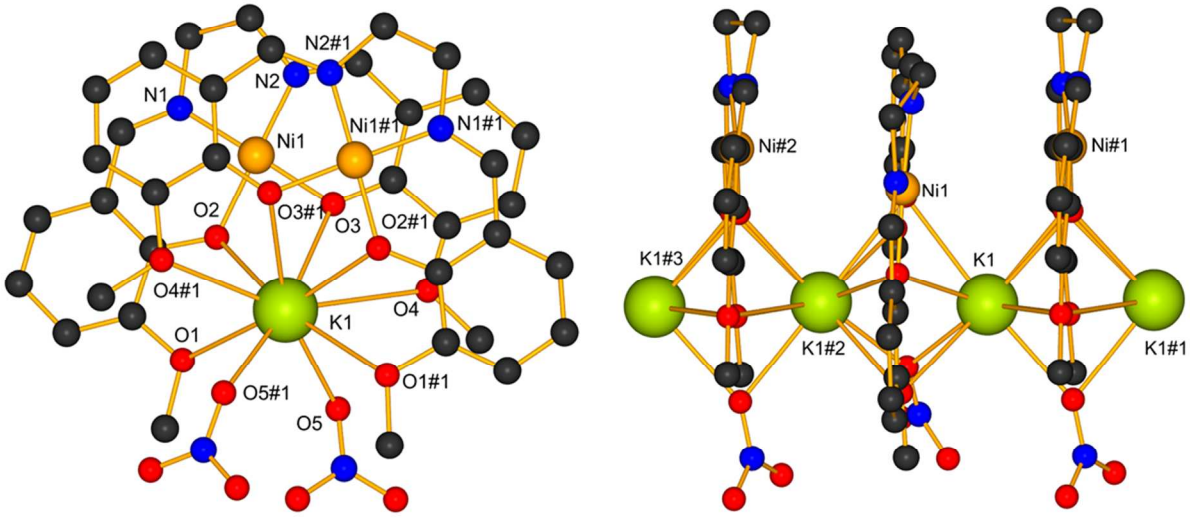

Figure S33 : Crystal structure of LNiK complex 8, the pentagonal antiprismatic coordination of the potassium ion and the 1D-coordination polymer formations. All H-atoms were been omitted for more clarity.

LCuRb (4) and LCuCs (5)

[LCuRb(μ-NO_3)]$_n$ and **[LCuCs(μ-NO_3)]$_n$.** The following compounds **LCuRb** (**4)** and **LCuCs** (**5)** are in principle similar and crystallize both in the monoclinic space group $P2_1/n$ (No.14) with a 1:1:1 complex of L:Cu:Rb or **L**:Cu:Cs in the asymmetric unit. Single crystals of complex **4** are formed as green needles by slow evaporation of an ACN/EtOH solution of **LCuRb**, while single crystals of **5** are obtained as purple needles by slow vapor diffusion of Et_2O into an ACN/EtOH solution of **LCuCs**. The Cu(II) is in both cases coordinated in an octahedral fashion with a perfect square planar base by the N_2O_2 chelating moiety of the ligand with Cu–O distances of 1.912(2) and 1.899(2) for O2 and O3, respectively, of the phenolate moieties of **4** and 1.903(3) and 1.901(3) for **5** and Cu–N distances of 1.927(2) and 1.934(2) Å for N1 and N2, respectively, of the imine groups for **4** and 1.925(4) and 1.929(4) Å for **5**, leading to angle sums of 360.18° for **4** and 360.2° for **5**. The coordination is for both compounds completed by the O5#3 and O6#5 oxygen atoms of two different nitrate anions with 2.638(3) Å and 2.825(3) Å for **4** and O5#4 and O6#1 with 2.844(4) Å and 2.962(4) Å for **5**, indicating the presence of a Jahn-Teller effect. The rubidium ion in **4** is coordinated by two O_2O_2 coordination sites of neighboring ligands, involving the phenolate oxygen atoms O2, O3, O2#3, O3#3 with Rb-O distances of 2.849(2), 2.877(2), 2.892(2) and 2.847(2) Å and the methoxides O4 and O4#3 oxygen atom with Rb-O distances of 3.035(2) and 3.416(2) Å. Its tenfold coordination completed by the O5, O6 and O6#3 from the nitrate ion which acts as bridging ligand towards a rubidium ion of the next neighbor complex, generating thus a one-dimensional (1D) coordination polymer along the *b*-axis.
Compound **5** adopts a similar structural motif but with Cs(I) instead of Rb(I). The decahedral coordination sphere of the alkali metal ion includes the phenolate oxygen atoms, O2, O3, O2#1, and O3#1 with Cs-O distances of 3.037(3), 2.981(3) 3.022(3) and 3.288(3) Å, respectively, as well as the methoxide oxygen donors O1, O4, O1#1, and O4#1 with distances of 3.108(4), 3.226(3), 3.641(4) and 3.040(3) Å, respectively. Again, the coordination sphere is completed by O5, O5#1 and O6 from two nitrate ions with 3.214(4) Å, 3.259(4) Å and 3.266(4) Å, both of which act as bridging entities towards cesium ions of the next neighbor complex, leading again to the characteristic one-dimensional (1D) coordination polymer along the *b*-axis.

The distances between the rubidium ion and the mean plane formed by the Cu(II) ion and the N_2O_2 are 1.688 Å and 1.879 Å on each side. For the cesium compound, these distances are 1.493 Å and 2.207 Å on each side of the plane, showing a stronger asymmetry and distortion than the rubidium compound. The distance between neighbor rubidium respectively cesium ions, within the coordination polymer chain is then 3.578(4), respectively 3.764(4) Å. In both crystal structures **4** and **5**, the **LCu** moieties are alternatingly arranged at 180° to each other and perpendicular with respect to the chain propagation direction along the crystallographic *b*-axis.

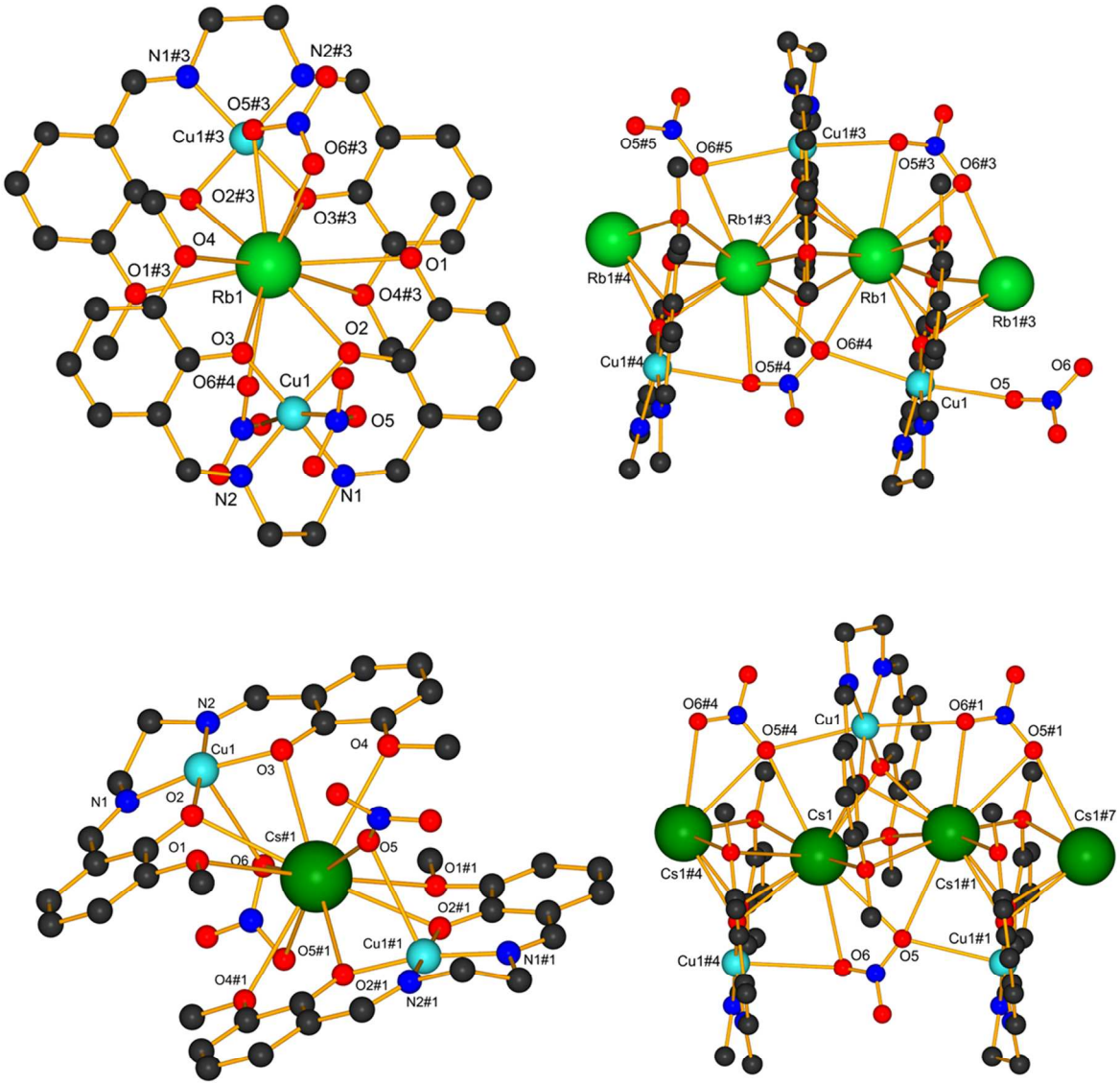

Figure S34: Crystal structure of LCuRb (4) and LCuCs (5) complex, and their 1D-structure coordination polymers. All H-atoms were been omitted for more clarity.

LNiRb (9)

[(LNiRb(NO$_3$)]$_n$. The following LNiRb compound 9 crystallizes in the monoclinic space group *P*2$_1$/a (No.14), respectively, with a 1:1:1 complex in the asymmetric unit. Single crystals of both complexes are formed as orange needle by slow evaporation of an ACN/EtOH solution of 9. The Ni(II) ion is in both cases coordinated in a square planar fashion by the N_2O_2 chelating moiety of the ligand with Ni–O distances of 1.853(3) and 1.850(2) for O2 and O3, respectively, of the phenolate moieties for LNiRb and Ni–N distances of 1.846(4) and 1.849(3) Å for N1 and N2, respectively, of the imine groups for LNiRb. The angle sum around the nickel ions sum up to 360.12° with Rb(I), indicating the planarity of the coordination. The rubidium ion in 9 is coordinated by two O_2O_2 coordination sites of neighboring ligands involving the phenolate oxygen atoms O2, O3, O2#2, O3#2 with Rb-O distances of 3.045(3), 2.963(3), 2.996(3) and 2.984(3) Å and the methoxide oxygen donors O1, O1#2, O4 and O4#2 with Rb-O distances of 3.120(3), 3.12(3), 3.131(3) and 3.107(3) Å, respectively. Its coordination sphere is completed by O5 and O5#2 from two nitrate ions which act as bridging ligands towards the next neighbor rubidium ions, generating thus a one-dimensional (1D) coordination polymer along the *a*-axis. The distances between the rubidium ion and the mean plane formed by the Ni(II) ion and the N_2O_2 are 1.731 Å and 1.871 Å on each side and shows that the metal ion is entirely out of plane. The distance between neighbor rubidium and cesium ions, respectively, within the sequence is then 3.612(7). In contrast to the Cu-compounds, but similar to the LNiK compound, the ligand is all arranged on the same side of the 1D polymer chain propagation direction, and is offset by 41.79° with respect to each other.

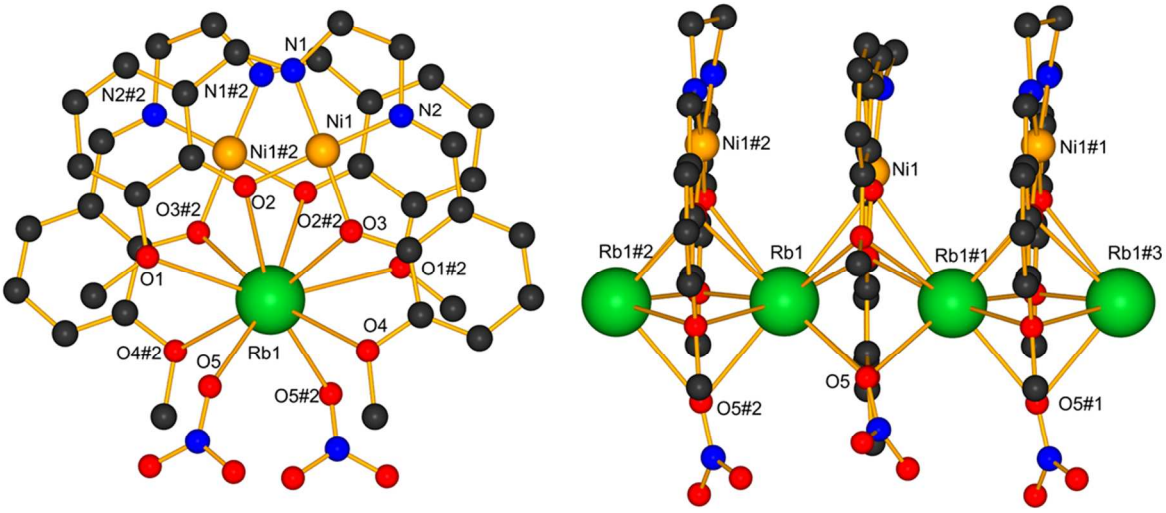

Figure S35 : Crystal structure of LNiRb complex 9, and their 1D-structure coordination polymers. All H-atoms were been omitted for more clarity.

(LNi)$_2$Cs (10)

[{(LNi)$_2$Cs(NO$_3$)}(CHCl$_3$)]$_n$. The following compounds (LNi)$_2$Cs (10) crystallize in the monoclinic space group *P*2$_1$/c (No.14), with a 1:1:1 complex in the asymmetric unit. Single crystals of both complexes are formed as orange needle by slow evaporation of an ACN/EtOH solution of 10. The Ni(II) ion is in both cases coordinated in a square planar fashion by the N_2O_2 chelating moiety of the ligand with Ni–O distances of 1.584(2) and 1.545(2) for O2 and O3, and 1.842(2), 1.846(2) respectively for O6 and O7 of the

phenolate moieties for $(LNi)_2Cs$ and Ni–N distances of 1.847(2) and 1.843(2) Å for N1 and N2, 1.848(2) and 1.841(2) for N3 and N4, respectively, of the imine groups for LNiCs. The angle sum around the nickel ions sum up to 360.2° with Cs(I), indicating the planarity of the coordination. The cesium ion in 10 is coordinated by two O_2O_2 coordination sites of neighboring ligands involving the phenolate oxygen atoms O2, O3, O6, O7 with Cs-O distances of 1.584(2), 1.545(2), 3.032(2) and 3.099(2) Å and the methoxide oxygen donors O1, O4, O5 and O6 with Cs-O distances of 3.156(2), 3.063(2), .139(2) and 3.223(2) Å, respectively. Its coordination sphere is completed by O9 and O10 from two nitrate ions with a distance Cs–O of 3.207(3) and 3.309(3) Å which act as bridging Ni-ligands towards one cesium ion, generating thus a sandwich conformation $(LNi)_2Cs$. The distances between the cesium ion and the mean plane formed by the Ni(II) ion and the N_2O_2 are 1.399 Å and 1.782 Å on each side and shows that the metal ion is entirely out of plane. As for the analogous Cu-compounds, the Cs-ion is coordinated in a more asymmetric way by the ligands H_2L.

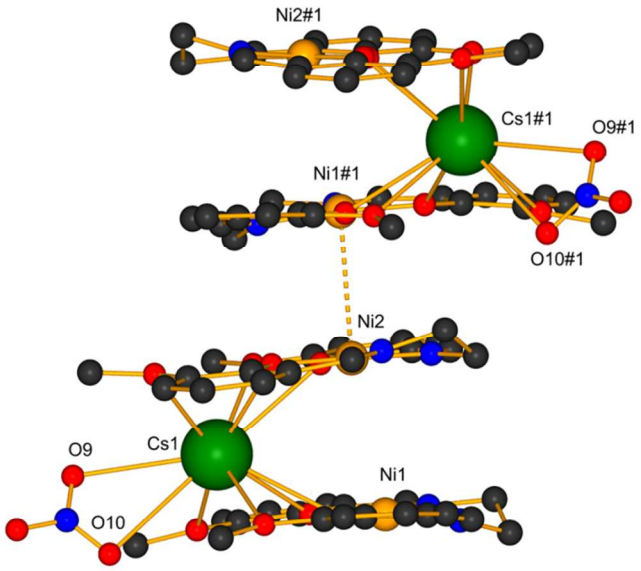

Figure S36 : Crystal structure of $(LNi)_2Cs$ complex 10, and their 1D-structure coordination polymer. All H atoms were been omitted for more clarity.

Comparison. Several similarities and differences between the nickel and copper complexes have been observed. Due to the use of these two transition metal ions, every compound adopts a square planar motif in the N_2O_2 region. It was shown that the Schiff base compartment pocket much better nickel(II) metal ion than copper(II) which tends to form an octahedral coordination sphere using nitrate ions. Indeed, the distance between the transition metal ion M_1 and the N_2O_2 plane show clearly that copper(II) seeks to be out of the plane with distances oscillating between 0.019-0.076 Å while nickel(II) while fit almost perfectly in the N_2O_2 cavity with a distance between 0.001-0008 Å, depending of the alkali used. Each complexes crystallize in a 1:1:1 stoichiometry for $L:M_1:M_2$. Li(I) and Na(I) compounds form discreet structures while those containing K(I), Rb(I) and Cs(I) form 1D coordination polymers. Furthermore, these last three complexes show the alkali metal ions more and more out of the M_1 plane due to the gradual increase of the size of their radii. These different 1D coordination polymers adopt two conformations

depending on the transition metal ion used. Those containing nickel(II) metal ion as M_1 exhibit a face to face stacking along the axis while those synthetized with copper(II) metal ion show a helical morphology along the axis by dint of the nitrate moieties giving a octahedral coordination to the copper.
It was shown that in the copper complexes, the copper(II) possess a close link with the nitrate ions in the different structures. This might explain the color change of the compounds as one goes down the list of the alkali metals. In fact, Li(I) complex shows a quasi-perfect elongated distortion with equivalent axial bond distances which can this strong purple color. Na(I) compounds can be considered as a fivefold Jahn Teller effect where the square pyramidal geometry of the cooper is distorted due to the elongation of the axial bond with the nitrate ion. On the other hand, K(I), Rb(I) and Cs(I) complexes produce a much more light color and this can be explain by the fact that their axial bond distances of the Jahn-Teller distortion are not more equivalents. Indeed, the length of such bond can differ between 1.118 to 0.187 Å.

$[(LCuLi(NO_3))_2(\mu\text{-}H_2O)]$ (1') and $[\{LCuNa(NO_3)\}_3]_n$ (2').
While obtaining the analogous LNiLi structure to 1 with an additional water molecule failed, we could obtain the Cu-containing structure analogous to 6 with only one water molecule, namely [(LCu-Li(NO_3))$_2$(μ-H_2O)] (1'). The connectivities are similar as in 6 with a torsion angle Cu1–Li1–Li2–Cu2 of ca. 47° within a "dimer" and Cu1–C31 as well as Cu1–C32 contacts shorter than 3.3 Å between two dimers. While in 1', the dimers arrange antiparallel to each other along the *a*-direction as in 6, the connectivity along the *c*-direction is mainly governed by H-bonds shorter than 2.7 Å between the O18 of a nitrate anion and H11 and H13 of a neighbor entity.
Suitable crystals of the complex LCuLi (1') with the nickel (II) ion coordinated as M_1 in the imine-based N_2O_2 site have been obtained as dark green block-like crystals by slow vapor diffusion of Et_2O into an ACN/EtOH solution containing the redisolved compound from ether precipitation. In contrast to 1, the compound crystallizes in an orthorhombic *P*bca space group (No. 61) in a 1:1:1 stoichiometry for L:Cu:Li. Like for 1, two non-equivalent entities are present in the unit cell as L1:Cu1:Li1 and L2:Cu2:Li2. The transition metal ion is coordinated in a square planar fashion by the N_2O_2 chelating moiety of the ligand with Cu–O distances of 1.989(3) and 1.884(4)Å for O2 and O3 (Cu1), 1.877(3) and 1.887(3) Å for O6 and O7 (Cu2) of the phenolate moieties and Cu–N distances of 1.915(4) and1.910(4) Å for N1 and N2 (Cu1), respectively, 1.910(4) and 1.914(4) Å for N3 and N4 (Cu2) of the imine groups. The angle sums around the nickel ions are 360.02°(Cu1) and 360°(Cu2), indicating the better planarity of the coordination for complex 1' than for 1. In contrast to 1, the cavity formed by the O_2O_2 coordination site is now centrally occupied by a lithium ion, linking only the two phenolate oxygen atoms O2 and O3 for Li1 or O6 and O7 for Li2 with Li-O distances 2.078(8) and 2.071(9) Å, respectively 2.025(9) and 2.025(9)Å. O1 and O4 as well as O5 and O6 are not coordinated to Li1 and Li2, respectively as in his analogue structure LNiLi (6) . The distance between the lithium ion and the mean plane formed by the Cu(II) ion and the N_2O_2 is 0.047 Å for Cu1 or 0.049 Å for Cu2 and shows that the alkali metal ion is practically in plane with LCu. Further coordination to the lithium ions occurs via O9 (Li1) and O12 (Li2) of nitrate ions with distances of 2.054(9) Å and 1.98(1) Å respectively and a bridging water molecule O15 between the two alkali metal ions with distances of 1.954(8) Å (Li1) and 2.00(1) Å (Li2). In contrast to 1 and equivalent to 6, no one-dimensional chain is formed by bridging water molecules. Instead, a short contact between the Cu(II) and the π-system of the neighbor complex allows an expansion along the *a*-axis. The distance between neighbor lithium ions within the sequence is then 3.30(1) Å (Li1–Li2).
Between the three complexes, the copper ions are also involved in contacts between Cu2 and three C-atoms of the π-system of the complex containing Cu1, while on the other side; Cu2 is weakly coordinated by the ether oxygen O9. Cu1 and Cu3 are weakly π-coordinated by C21 and C22, respectively by C30, C31 and C32.

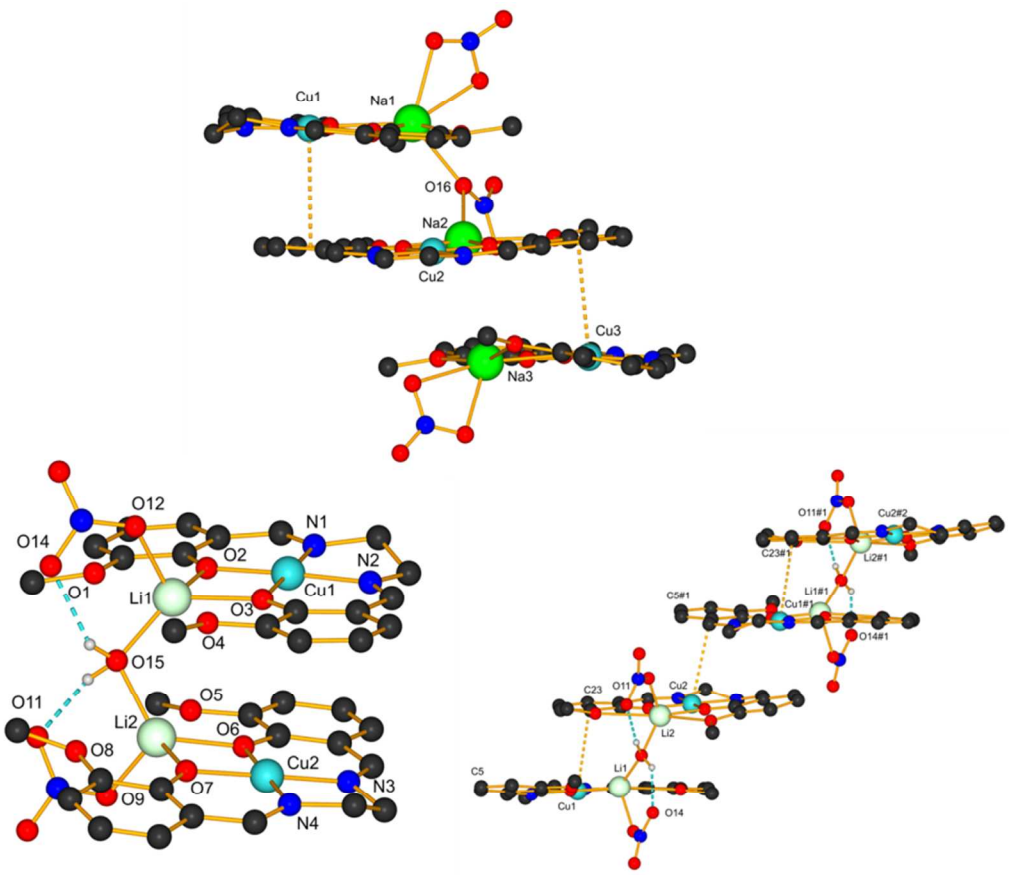

Figure S37: Crystal structure of LCuNa complex 2’ (above) and LCuLi complex 1’ (below) with its correspondent short contacts and H-bonds. Partial H-atoms are omitted for clarity.

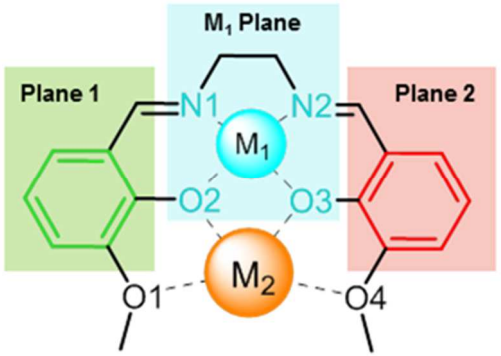

Schema S2: Representation of the different planes.

Table S1 : Bonds lengths and angles of all crystal structures obtained.

Compounds No.	**Ionic radii M_2 (Coord. No.)**	**Plane 1/ Plane 2**	**Plane 1/ Cu Plane**	**Plane 2/ Cu Plane**	**Cu Plane/ M_2**	**N_2O_2 Plane-Cu**	**Cu–M_2**	**M_2–M_2**
1	59 pm(4)	4.30° and 4.80°	9.70° and 11.91°	10.1°5 and 9.25°	0.272 and 0.195 Å	0.060 and 0.033 Å	3.480(4) and 3.461(4) Å	3.506(7)/ 3.484(6) Å
1'	59 pm(4)	8.11° and 5.05°	1.32° and 6.91°	8.06° and 4.49°	0.047 and 0.049 Å	0.016 and 0.003 Å	3.032(8) and 2.950(9) Å	3.30(1) Å
2	102 pm(6)	14.56°	15.38°	2.63°	0.156 Å	0.025	3.335(2) Å	-
2'	102 pm(6)	3.39° and 6.70° and 9.60°	4.64° and 4.30° and 5.64°	1.94° and 3.55° and 8.27°	0.188 and 0.057 and 0.149 Å	0.009 and 0.000 and 0.012 Å	3.375(2) and 3.221(6) and 3.266(6) Å	3.926(8) and 5.988(8) Å
4	173 pm(10)	5.17°	8.99°	8.37°	1.688 and 1.879 Å	0.019 Å	3.674(4) and 3.632(4) Å	3.578(4) Å
5	188pm(10)	15.22°	6.66°	12.2°7	1.493 and 2.207 Å	0.076 Å	3.873(6) and 3.743(6) Å	3.764(4) Å

Compounds No.	**Ionic radii M_2 (Coord. No.)**	**Plane 1/ Plane 2**	**Plane 1/ Ni Plane**	**Plane 2/ Ni Plane**	**Ni Plane/ M_2**	**N_2O_2 Plane-Ni**	**Ni–M_2**	**M_2–M_2**

6	74 pm(6)	9.18 and 5.42°	2.33° and 5.86°	8.48° and 8.25°	0.021 and 0.043 Å	0.002 and 0.004 Å	2.010(7) and 2.986(5) Å	3.406(9) Å
7	102 pm(6)	5.87°	4.17°	3.84°	0.221 Å	0.008 Å	3.390(2)	-
7'	102 pm(6)	7.65°	3.15°	4.60°	0.004 Å	0.004 Å	3.368(7) Å	-
8	160 pm(10)	8.24°	5.36°	9.37°	0.875 and 1.675 Å	0.002 Å	2.800(9) and 3.741(8) Å	3.558(1) Å
9	173 pm(10)	6.44°	8.56°	5.12°	1.731 and 1.871 Å	0.004 Å	3.895(7) and 3.830(7) Å	3.612(7) Å
10	188 pm(10)	6.43 and 1.52°	8.36° and 7.77°	6.04° and 9.23°	1.399 and 1.782 Å	0.004 and 0.001 Å	3.945(6) and 4.083(6) Å	-

Distance Å	**LCuLi 1**	**LCuLi 1'**	**LCuNa 2**	**LCuNa 2'**	**LCuRb 4**	**LCuCs 5**
N1–Cu1/Cu1–N2	1.948(2)/1.941(2)	1.915(4)/1.910(4)	1.915(3)/1.922(3)	1.91(9)/1.99(2)	1.927(2)/1.934(2)	1.925(4)/1.929(4)
N3–Cu2/Cu2–N4	1.960(2)/1.937(2)	1910(4)/1.914(4)	-	2.90(2)/1.93(1)	-	-
N5–Cu3/Cu3–N6	-	-	-	1.90(1)/1.92(1)	-	-
O2–Cu1/Cu1–O3	1.915(2)/1.928(2)	1.989(3)/1.884(4)	1.900(3)/ 1.882(3)	1.91(1)/1.88(1)	1.912(2)/1.899(2)	1.903(3)/1.901(3)
O6–Cu2/Cu2–O7	1.905(2)/1.938(2)	1.877(3)/1.887(3)	-	1.910(9)/1.92(1)	-	-
O10–Cu3/Cu3–O11	-	-	-	1.87(1)/1.895(9)	-	-
O1–M_2/M_2–O4	-/2.029(4)	-	2.723(4)/ 2.552(4)	2.71(1)/2.59(1)	-/3.035(2)	3.108(4)/3.226(3)
O1#–M_2/M_2–O4#	-	-	-	-	-/-	-/3.040(3)
O2–M_2/M_2–O3	-/2.073(4)	2.078(8)/2.071(9)	2.383(4)/2.306(4)	2.36(19/2.36(1)	2.849(2)/2.877(2)	3.037(3)/2.981(3)
O2#–M_2/M_2–O3#	-	-	-	-	2.892(2)/2.847(2)	3.022(3)/3.288(3)
O5–M_2/M_2–O8	-/2.049(4)	-	-	2.65(1)/2.64(1)	-	-
O6–M_2/M_2–O7	-/2.086(4)	2.025(9)/2.025(9)	-	2.22(1)/2.21(1)	-	-
O9–M_2/M_2–O12	-	-	-	2.63(1)/2.74(1)	-	-
O10–M_2/M_2–O11	-	-	-	2.27(1)/2.31(1)	-	-

LCuLi (1) : #1 (1+x, y, z), **LCuLi (1')** : #1 (½ +x, y, ½ - z), **LCuNa (2)**: #1(-1+x, y, z), #2(1+x, y, z), #3(½ -x, 1-y, ½+z),,#4($^3/_2$ -x, 1-y, - ½ +z), **LCuRb (4)** : #3(½ -x, ½+y, ½-z), #4(x, 1+y, z), #5(½ -x, $^3/_2$ +y, ½-z), **LCuCs (5)** : #1(½ -x, ½+y, ½-z), #4(½ -x, - ½ +y, ½-z), #7(x, 1+y, z).

Distance Å	**LNiLi 6**	**LNiNa 7**	**LNiNa(MeOH) 7'**	**LNiK 8**	**LNiRb 9**	**LNiCs 10**
N1–Ni1/Ni1–N2	1.835(2)/1.840(2)	1.841(4)/1.843(3)	1.844(2)/1.836(1)	1.842(3)/1.839(2)	1.846(4)/1.849(3)	1.847(2)/1.843(2)
N3–Ni2/Ni2–N4	1.844(2)/1.843(2)	-	-	-	-	1.848(2)/1.841(2)
O2–Ni1/Ni1–O3	1.844(2)/1.838(2)	1.843(3)/1.845(3)	1.840(1)/1.833(1)	1.847(2)/1.852(2)	1.853(3)/1.850(2)	1584(2)/1.545(2)
O6–Ni2/Ni2–O7	1.842(2)/1.852(2)	-	-	-	-	1.842(2)/1.846(2)
O1–M_2/M_2–O4	2.570(7)/2.605(7)	2.546(3)/2.550(3)	2.362(2)/2.325(1)	3.071(3)/-	3.120(3)/3.131(3)	3.156(2)/3.063(2)
O1#–M_2/M_2–O4#	-	-	-	-/2.887(2)	-/3.107(3)	-
O2–M_2/M_2–O3	1.984(7)/2.010(7)	2.360(3)/2.369(3)	2.536(2)/2.458(1)	2.917(2)/2.919(2)	3.045(3)/2.963(3)	3.099(2)/3.136(2)
O2#–M_2/M_2–O3#	-	-	-	2.936(2)/3.055(3)	2.996(3)/2.984(3)	-
O5–M_2/M_2–O8	2.542(7)/2.677(6)	-	-	-	-	3.139(2)/3.223(2)
O6–M_2/M_2–O7	1.989(5)/2.041(7)	-	-	-	-	3.032(2)/3.099(2)
O9–M_2/M_2–O10	-	-	-	-	-	3.207(3)/3.309(3)
O5–Na1/O7–Na1/O8–Na1	-	-	2.544(2)/2.461(2)/ 2.376(2)	-	-	-

LNiLi (6): **#1** (½ +x, y, ½-z), **LNiNa (7)**: **#1**(1+x, y, z), **#2**(-1+x, y, z), **LNiNa(MeOH) (7')**: **#1**(-1+x, y, z), **#2**(-x,-y,-z), **#3**(1-x, -y, -z), **LNiK (8)**: **#1**(x, - ½ -y, - ½ +z), **#2**(x, - ½ -y, ½+z), **#3**(x, y, 1+z), **LNiRb (9)** : **#1**(½ +x, ½-y, z), **#2**(- ½ +x, ½-y, z), **#3**(1+x, y, z), **$(LNi)_2Cs$ (10)** : **#1**(x, ½-y, ½+z).